1. Introduction

The numerical treatment of many-body problems in solid state physics belongs to the realm of computer physics. Computer physics has evolved from 'number crunching' and 'dump data plotting' into a competitive field on a par with experimental an theoretical physics strongly entwined with both. Real experiments can be replaced by computer experiments as it is common practice in industry for monetary reasons. On the premises that an appropriate is simulated, the numerical experiment is often much faster, less expensive and in some cases even the only feasible alternative. With little extra effort, system parameters can be modified and novel material synthesized and the respective properties investigated.

As far as the links to theoretical physics are concerned the situation is similar. Computer physics has been disdained for many years by the 'pure theorists' claiming numerical results provide numbers and no insights. The situation has drastically changed over the last decade as testify by the significant and still increasing fraction of publications based essentially on computational techniques. Computer simulations from the theoretical viewpoint allow to scrutinies different models to figure out which fits the data best. Parameters can be modified with ease investigating wide parameter regimes with one and the same method. Otherwise different approaches have to be tailored for different parameter regimes, like week coupling strong-coupling etc.

A widely used approach is the density functional theory in various guises. The most famous approximation is the Local density approximation with various approximations to the unknown exchange-correlation potential. By definition, these one-particle approaches describe weekly correlated systems. Strongly correlated many-body systems are defined as those in which the simultaneous presence of all particles is essential for the respective phenomena. DFT is in principle exact in the sense that These techniques will not be discussed here.

revealing why numeric fast more than number crunching exact sometimes only approach generally applicable leichter bertragbar auf industrial applications no expert needed who spends months or even years solving one problem

2. Many Body Hamiltonians

The genuine ab-initio Hamiltonian describing condensed matter is the ab-initio Hamilton operator containing in the Oppenheimer-approximation. It forms the starting point for bandstructure calculations in the local-density-approximation (LDA), in which electronic correlations are treated on a mean-field level. The realm of LDA calculations are weakly correlated systems, as opposed to strongly correlated electronic systems in which the detailed electron-electron-interaction is responsible for correlation effects such as anti-ferromagnetism, Kondo-effect, fractional quantum-hall effect, Mott-transition and many more.

An exact treatment of ab-initio many-body problems is illusory. There are two options, either we stick to the ab-initio many-body Hamiltonian and are satisfied with uncontrolled approximations or we resort to model Hamiltonians which hopefully still contain the crucial essentials of the sought-for physical effect.

Model systems have the advantage that they can either be solved exactly by analytical means or they can be approached by numerical techniques. Numerical techniques are often the only feasible and reliable method for studying the really tough and long-standing problems of such systems.

We will begin with a concise description of the most important Hamilton operators for strongly correlated quantum systems, which have been the subject of intense numerical studies over the last 1-2 decades.

2.1 Hubbard model

We start out with the good old Hubbard model [1, 2] a simple model for interacting electrons in narrow bands. Assuming localized orbitals and a strong screening of the Coulomb interaction, only the local density-density repulsion is allowed for. The mere on-site interaction is certainly a crude approximation to the Coulomb interaction, but, for certain phenomena, it bears already the essential features of strongly correlated electrons. The Hubbard model was originally introduced to study the metal-insulator transition and ferromagnetism of itinerant electrons in narrow bands. During the last decade it has re-gained considerable attention in connection with the high temperature superconductors.

Possible realizations of this model are atoms with partially filled 3d-shells. In these systems the physics at the Fermi-level is governed by electrons in localized (3d-) orbitals. The model is defined by

$$H = \underbrace{-t \sum_{\substack{\langle i,j \rangle \\ \sigma}} a^\dagger_{i\sigma} a_{j\sigma}}_{H_0} \underbrace{+U \sum_i n_{i\downarrow} n_{i\uparrow}}_{H_1} -\mu \hat{N} \ , \tag{2.1}$$

where $a^\dagger_{i\sigma}(a_{i\sigma})$ create (annihilate) fermions of spin $\sigma =\uparrow,\downarrow$ in a Wannier orbital centered at site i. $n_{i\sigma}$ denotes the occupation number operator $n_{i\sigma} = a^\dagger_{i\sigma} a_{i\sigma}$. The electrons move in tight binding bands, with a transfer integral t between nearest neighbor sites, as indicated by $\langle i,j \rangle$. The strength of the Coulomb interaction is U. The number of lattice-sites will be denoted by N. If not stated otherwise the underlying lattice will be "simple cubic" in 1-D, 2-D, or 3-D. For $U \gg t$ double-occupancies are energetically unfavourable. The dominant contributions to the low-lying eigenstate are those real-space configurations in which there are as few double-occupancies as possible. Of particular physical interested is the situation near half-filling. At half-filling there are as many electrons as there are site, namely N. Both spin directions get their equal share. The energetically favoured configurations are those with one electron per lattice site. The charge movement his hampered by a potential energy barrier of hight U. Unless there an applied voltage does not overcome this threshold there will be no significant current. The system is insulating. The reasons is merely the on-site Coulomb repulsion. Without U the system would be a perfect metal at half-filling. The same energy gap shows up in inverse photoemission. To bring an extra electron into the system an additional energy U has to be paid. In the insulating state only the spin degrees of freedom are dynamic and it can be shown in second order perturbation theory that the Hubbard model maps onto an Heisenberg model with antiferromagnetic nearest-neighbor spin-spin interaction.

For grand canonical calculations, in (2.1) a chemical potential μ is included which couples to the particle-number operator

$$\hat{N} = \sum_i n_{i\downarrow} + n_{i\uparrow} \ . \tag{2.2}$$

Besides the on-site repulsion some applications also include nearest-neighbor density-density repulsion, as well, or even long-ranged density-density interactions. The model

$$H = H_{\text{Hubbard}} + V \sum_{\langle ij \rangle} n_i n_j$$

is called the extended Hubbard model. We will also be interested in the negative-U (attractive) Hubbard model

$$H = -t \sum_{\langle i,j \rangle\ \sigma} a^\dagger_{i\sigma} a_{j\sigma} - |U| \sum_i \big(n_{i\downarrow} - \frac{1}{2}\big)\big(n_{i\uparrow} - \frac{1}{2}\big) - \mu \hat{N}$$

In this notation the chemical potential vanishes at half-filling $\langle n \rangle = 1$ which follows immediately from the invariance under particle-hole transformation. Particularly useful is the asymmetric particle-hole transformation

$$\begin{aligned} a^\dagger_{i\uparrow} &\to a^\dagger_{i\uparrow} & a_{i\uparrow} &\to a_{i\uparrow} \\ a^\dagger_{i\downarrow} &\to e^{i\boldsymbol{Q}\boldsymbol{x}_i} a_{i\downarrow} & a_{i\downarrow} &\to e^{-i\boldsymbol{Q}\boldsymbol{x}_i} a^\dagger_{i\downarrow} \end{aligned} \tag{2.3}$$

with $\boldsymbol{Q} = (\pi, \ldots, \pi)$. Equation (2.3) leaves the nearest neighbor hopping term of the Hamiltonian invariant, changes the sign of the onsite-Hubbard interaction and introduces a homogeneous magnetic field in z-direction

$$H \longrightarrow H_0 + |U| \sum_i \big(n_{i\downarrow} - \frac{1}{2}\big)\big(n_{i\uparrow} - \frac{1}{2}\big) - \mu \sum_i \underbrace{\big(n_{i\uparrow} - n_{i\downarrow}\big)}_{2\sigma^z_i} - \mu N \; . \tag{2.4}$$

Hence, the negative-U model maps onto the repulsive Hubbard model in a homogeneous magnetic field of strength $h = 2\mu$. The latter vanishes only at half-filling. Interesting consequences of (2.3) are

$$\begin{aligned} \Delta^\dagger_i &= a^\dagger_{i\uparrow} a^\dagger_{i\downarrow} &\longleftrightarrow\quad & e^{i\boldsymbol{Q}\boldsymbol{x}_i} a^\dagger_{i\uparrow} a_{i\downarrow} = e^{i\boldsymbol{Q}\boldsymbol{x}_i} \sigma^+_i \\ \Delta_i &= a_{i\downarrow} a_{i\uparrow} &\longleftrightarrow\quad & e^{-i\boldsymbol{Q}\boldsymbol{x}_i} a^\dagger_{i\downarrow} a_{i\uparrow} = e^{-i\boldsymbol{Q}\boldsymbol{x}_i} \sigma^-_i \\ n_i &= n_{i\uparrow} + n_{i\downarrow} &\longleftrightarrow\quad & n_{i\uparrow} - n_{i\downarrow} + 1 = 2\sigma^z_i + 1 \end{aligned} \tag{2.5}$$

$\sigma_i^{(+,-,z)}$ are the Pauli matrices. Equation (2.5) can be used to deduce results for the negative-U Hubbard model from those of the repulsive one. For instance the staggered magnetization in x,y- direction in the repulsive case maps onto pair-field operators Δ_i and the staggered magnetization in z-direction translates into charge-density waves. Since at half-filling the repulsive Hubbard model in 2d exhibits long-ranged antiferromagnetic order at T=0K, there is a coexistence of superconductivity and charge-density waves in the attractive model.

2.2 Emery model

An extension of the Hubbard model is the three-band Hubbard model (or Emery model)[3]. It is particularly geared for the high temperature copper-oxide superconductors. The low-lying excitations of these systems are predominated by the Cu(3d) and O(2p) orbitals, stemming from a two-dimensional arrangement of copper and oxygen atoms. The copper-atoms form a simple-cubic lattice. Half way between nearest-neighbor copper sites there is a oxygen atom. Only the three most relevant orbitals are taken into account. The Hamilton operator is formally similar to that of the Hubbard model

$$H = \underbrace{\sum_{\langle i,j\rangle\ \sigma} t_{ij} a^\dagger_{i,\sigma} a_{j,\sigma}}_{H_0} + \underbrace{\sum_i U_i n_{i\downarrow} n_{i\uparrow}}_{H_{\mathrm{Hubb}}}$$

The compound indices i and j include the unit cell index and the index for the orbitals within the unit cell (Cu, O_1, O_2). Again, only a local Coulomb-interaction is taken into account, with different parameters for copper and oxygen orbitals U_d and U_p, respectively. The hopping processes involve neighboring oxygen-copper bonds and oxygen-oxygen bonds with the respective parameters t_{pd} and t_{pp}.

2.3 The t-J model

The t-J model consists of a constraint hopping term for the charge degrees of freedom, allowing no double occupancies. It can be derived as strong U limit of the Hubbard model. In the restricted space the eliminated double occupancies result in an effective spin-spin interaction

$$H = t \sum_{\langle i,j\rangle\ \sigma} \big(1 - n_{i,-\sigma}\big) a^\dagger_{i,\sigma} a_{j,\sigma} \big(1 - n_{j,-\sigma}\big) + J \sum_{\langle i,j\rangle} \big(\boldsymbol{S}_i \boldsymbol{S}_j - \frac{n_i n_j}{4}\big)\ . \quad (2.6)$$

The projection operators $(1 - n_{i,-\sigma})$ in the kinetic term ensure that no site is occupied by more than two electrons. The spin operators at site i are $\boldsymbol{S}_i = \sum_{\sigma\sigma'} a^\dagger_{i\sigma}\ \boldsymbol{\sigma}_{\sigma\sigma'}\ a^\dagger_{i\sigma'}$, with $\boldsymbol{\sigma}_{\sigma\sigma'}$ being the Pauli matrices. S_i describes magnetic moments with S=1/2 for occupied sites and S=0 for empty sites.

(2.6) cannot only be derived from the Hubbard model but also approximately from the Emery model by virtue of the Zhang-Rice-construction[4]. For a review we refer to [5]. The tJ-model is being understood as a generic model for the interplay of charge- and spin degrees of freedom.

2.4 Anderson model

The Anderson impurity model was proposed in 1961 to explain the formation of local moments at a low concentration of transition metals in non-magnetic hosts [6]. The Anderson-lattice Hamiltonian[7] provides a natural generalization of the impurity model and is suited for the description of many transition-metal compounds, as well as rare-earth and actinide elements and compounds. Although many different approximation techniques have been applied, exact results are scarce. For an overview over the physics of the Anderson model we refer to [8, 9].

The specific model, studied in QMC calculations, involves two kinds of orbitals, which we call c and f here. In all QMC calculations to-date non-degenerate f-orbitals are assumed. The conduction band is again made up by nearest neighbor hopping processes and the Hamiltonian reads

$$H = \underbrace{t\sum_{\langle i,j\rangle\sigma} c^\dagger_{i,\sigma}c_{j,\sigma} + \sum_{i,j,\sigma} V_{ij}\big(c^\dagger_{i\sigma}f_{j\sigma} + f^\dagger_{i\sigma}c_{j\sigma}\big) + \varepsilon_f\sum_{i\sigma} n^f_{i\sigma}}_{H_0} + \underbrace{U\sum_i n^f_{i\downarrow}n^f_{i\uparrow}}_{H_{\text{Hubb}}}\,. \tag{2.7}$$

The quantity V is the hybridization-matrix element. The specific form of V is irrelevant for the time being. The transfer integral between nearest neighbor c-states is denoted by t, ε_f is the local potential of the un-hybridized single-particle f-orbital, and U is the f-electron interaction parameter. The c-atoms form a regular square lattice in 2-D or a simple cubic lattice. (2.7) describes both the Anderson-lattice model and the impurity model. In the latter cases sums over f-levels are restricted to the impurity sites. Since we need not to be more specific for the discussion of the QMC schemes we keep it in this handy form for the time being. Equation (2.7) can formally also be cast into the Emery-model, where the indices i and j account for unit cell and orbitals (c, f).

All Hamilton operators, discussed so far, have the same structure $H = H_0 + H_{\text{Hubb}}$, with a single-particle part H_0 and the local Hubbard interaction H_{Hubb}. Both constituents separately can be diagonalized with little effort. It is the interplay of both parts, which are diagonal in conjugate representations, that makes the Hubbard model such a tough problem. Because of the common structures these Hamilton operators can be treated within the same QMC scheme.

2.5 Heisenberg model

The Hubbard type models describe itinerant electrons. If the charge degrees of freedom are bound to the atomic positions only the spin degrees of freedom remain active. They are described by the Heisenberg hamiltonian, the fundamental model in the theory of magnetism of local magnetic moments. It is defined by

$$H = \sum_{i,j} J^z_{ij}S^z_iS^z_j + J^\perp_{ij}\left(S^x_iS^x_j + S^y_iS^y_j\right) + B\sum_i S^z_i \tag{2.8}$$

where S^α_i $(\alpha = x, y, z)$ is the α-th component of the spin-operator and J stands for the exchange integrals. The last term describes the coupling to an external magnetic field B in z-direction. This model is particularly geared for magnetic insulators like the 3d-,4d-,4f-,5f-systems.

There are several special cases of the Heisenberg model

- $J^z = J^\perp$ ... isotropic Heisenberg model
- $J^\perp = 0$ ... Ising model
- $J^z = 0$ ... XY-model

The spin operators obey the well known commutator algebra

$$[S_i^\alpha, S_j^\beta] = i\,\delta_{i,j}\,\epsilon_{\alpha\beta\gamma}\,S_i^\gamma \ .$$

For numerical purposes it is convenient to introduce ladder operators

$$S_i^\pm = S_i^x \pm i\,S_i^y \ .$$

Therefore, the operators S^x and S^y can be written as

$$S_i^x = \frac{1}{2}(S_i^+ + S_i^-) \quad , \qquad S_i^y = \frac{1}{2i}(S_i^+ - S_i^-) \ .$$

Instead of S^x and S^y we use the operators S^+ and S^- to express the Hamiltonian

$$H = {\sum_{ij}}' \left\{ J_{ij}\,S_i^z S_j^z + \frac{1}{2}\,J_{ij}^\perp \underbrace{(S_i^+ S_j^- + S_i^- S_j^+)}_{F_{ij}} \right\} + B \sum_i S_i^z$$

where the summation is restricted to $i \neq j$.

2.5.1 Spin 1/2 Heisenberg Antiferromagnet

The isotrope spin-1/2 Heisenberg antiferromagnet ($J < 0$) attracts particular interest as being the strong coupling limit of the Hubbard model at half-filling ($N_\uparrow = N_\downarrow = N/2$) with $J = -4t^2/U$ [10]. Moreover, it is governed by quantum effects more than any other spin system.

However, the perfectly ordered Neel-state $|\uparrow\downarrow\uparrow\downarrow\rangle$ is not the ground state of the system.

The Hamiltonian has the special form

$$H = -J \sum_{\langle ij \rangle} \left\{ S_i^z\,S_j^z + \frac{1}{2} F_{ij} \right\} \ .$$

We have used the common sign convention for the exchange-integral. In the antiferromagnic case J is negative. The spin-spin interaction is restricted to nearest-neighbor sites, indicated by $\langle ij \rangle$. The so-called flip operator F_{ij} has a simple meaning for spin-1/2 particles. It swaps the spin-values of the neighboring sites i and j, if the spins have opposite sign. Otherwise, the application of F_{ij} yields the null vector.

$$\hat{F}_{i,j}\,|\ldots,\sigma_i,\ldots,\sigma_j,\ldots\rangle = \begin{cases} |\ldots,-\sigma_i,\ldots,-\sigma_j,\ldots\rangle & \text{if } \sigma_i = -\sigma_j, \\ |0\rangle & \text{otherwise.} \end{cases} \ . \tag{2.9}$$

A gauge-transformation can be invoked to map the spin-1/2 Heisenberg Hamiltonian onto a hard-core boson system with repulsive nearest neighbor interaction [11]. This representation is useful from the numerical and analytical point of view [12]. The transformation is defined by $S_i^+ = b_i^+$, $S_i^- = b_i$ and $S_i^z = 1/2 - b_i^+ b_i$, with the hard-core constraint $b_i^{+^2} = 0$. For $J < 0$ and a bi-partite lattice it is favorable to perform an additional gauge transformation $b_i \rightarrow e_i \cdot b_i$, with e_i being 1 on one sublattice and -1 on the other. The hard-core boson Hamiltonian then reads

$$H = -J \sum_{<ij>} b_i^+ b_i + J \sum_{<ij>} n_i n_j + E_0 \ . \tag{2.10}$$

In the above equation, $E_0 = -Jz(N - N_b)/4$, with N_b being the number of bosons and z the number of nearest neighbors. N_b is related to the z-component of the total spin via $N_b = N/2 - S_0^z$. Both, N_b and S_0^z are conserved quantities. It has been shown that the ground state of (2.10) is nodeless and unique [13, 14].

2.5.2 Ising Model

The extrem unisotropic limit of the Heisenberg model is the Ising model, in which only the z-components of the spins are retained. Since no x- and y-components of the spins are involved, the Hamiltonian commutes with every S_i^z and the individual z-components are good quantum numbers. Therefore, the Ising model is a purely classical model, all operators commute and the only quantum-feature is the fact that only discrete values for S_i^z are allowed. The Hamiltonian of the Ising model reads

$$H = -J \sum_{<i,j>} S_i \, S_j + B \sum_i S_i \ , \tag{2.11}$$

where the spin-variables are restricted to ± 1. The Ising model is of particular interest for the theory of phase transitions since the 2d-Ising model has a second order phase-transition at a finite temperature and it can be solved analytically. There are various generalizations in the literature for a wide range of applications not only in physics but also in biology and in the field of pattern recognition. A particular class of generalizations leads to the so-called Potts-model. For a survey see [**?**].

2.5.3 The Potts Model

In the Potts–model the spins s_i can take on discrete values ranging from $1, 2, \ldots, q$. We restrict the discussion to periodic homogeneous systems where the Hamiltonian reads

$$H = -J \sum_{<i,j>} \delta_{s_i, s_j} \ . \tag{2.12}$$

As in the case of the Ising model, only nearest-neighbor spins interact and thus the sum is again restricted to nearest-neighbor sites i and j on the underlying lattice. Positive J values represent ferromagnetic coupling where, at $T = 0$, all spin values are equal. This ferromagnetic ground state is q-fold degenerate.

The Hamiltonian of the Potts model for $q = 2$ is related to that of the Ising model

$$H^I = -J^I \sum_{<i,j>} s_i \, s_j \tag{2.13}$$

via

$$\begin{aligned} H^I &= -J^I \sum_{<i,j>} \delta_{s_i,s_j} - (1 - \delta_{s_i,s_j}) \\ &= -2\, J^I \sum_{<i,j>} \delta_{s_i,s_j} + J^I \, N \, z \\ &= -J \sum_{<i,j>} \delta_{s_i,s_j} + J^I \, N \, z \, . \end{aligned} \tag{2.14}$$

Here, $J = 2\, J^I$ and z is the number of nearest neighbour pairs per lattice site. In the case of the Potts model, magnetic fields B couple via

$$H^1 = -B \sum_{i=1}^{N} \delta_{s_i,1} \tag{2.15}$$

where N denotes the number of spins. This formula relates to that for the Ising model via

$$\begin{aligned} H^{1I} = -B \sum_i s_i &= -B \sum_i \Big(\delta_{s_i,1} - (1 - \delta_{s_i,1}) \Big) \\ &= -2B \sum_i \delta_{s_i,1} + B\, N \, . \end{aligned} \tag{2.16}$$

Again, the coupling constant for the Ising model is twice that of the Potts model.

2.6 Kondo Model

The Kondo model was designed to describe the interaction of itinerant and localized (d, f) electrons of transition metal oxides such as $LaMaO_3$, which are presently the subject of intense investigations. Due to strong Hund's rule coupling, the localized electrons are in a high spin state, which results in This means that at every lattice site i there is a localized spins $\mathbf{S}_i$. The sites

i of these magnetic moments can either be distributed randomly to discribe magnetic impurities in metals or they can form a regular lattice. Like in the Hubbard model, the itinerant electrons are treated in the tight-binding approximation. They are subjected to strong exchange coupling with the localized spins. In its simplest form, the Kondo Hamiltonian reads

$$\hat{H} = -t \sum_{<i,j>,\,\sigma} a^{\dagger}_{i\sigma} a_{j\sigma} - J_H \sum_{i,\sigma,\sigma'} a^{\dagger}_{i\sigma'} \boldsymbol{\sigma}_{\sigma'\sigma} a_{i\sigma} \cdot \mathbf{S}_i \ . \tag{2.17}$$

Here, only one band of itinerant electrons is considered and electron–electron interaction are neglected. The coupling constant J_H has typical values of $J_H \approx 6$eV. Its influence is much greater than that of the hopping term.

Therefore, it is quite informative to consider the limit $J_H/t \to \infty$, where the itinerant spins are forced to align with the local ones. Then a misalignment of $\mathbf{S}_i$ and $\mathbf{S}_j$ suppresses the hopping, and, consequently a ferromagnetic ground state of the localized spins is favored. In this limit, an effective Hamiltonian can be derived. This is most easily done when considering the localized spins as classical vectors of equal length S pointing in the direction

$$\mathbf{n}_i = \ (\sin\theta_i \cos\varphi_i, \sin\theta_i \sin\varphi_i, \cos\theta_i) \ .$$

This simplification can be justified for large spins $S = 3/2,\ 5/2, \ldots$. In the case of classical localized spins, the effective Hamiltonian reads

$$H_{j_H=\infty} = -\sum_{<i,j>} t_{i,j}\, d^{\dagger}_{i\uparrow} d_{j\uparrow} \tag{2.18}$$

with a hopping integral $t_{i,j}$ now depending on the relative orientation of the neighboring spins

$$t_{i,j} = t\left[\cos(\theta_i/2)\cos(\theta_j/2) + \sin(\theta_i/2)\sin(\theta_j/2)e^{-i(\varphi_i-\varphi_j)}\right] \ .$$

The operators $d^{\dagger}_{i\uparrow}(d_{i\uparrow})$ generate (annihilate) itinerant electrons whose spins point in the direction of the localized spin $\mathbf{S}_i$. We see that $t_{i,j} = 0$ for anti-parallel spins ($\theta_i = \pi - \theta_j$ and $\varphi_i = \pi + \varphi_j$) and $t_{i,j} = t$ for parallel spins ($\theta_i = \theta_j$ and $\varphi_i = \varphi_j$).

Another strategy is to to integrate out the effects of the itinerant electrons. This procedure yields the so–called *double exchange Hamiltonian*. In case of $S = 1/2$ it is of the Heisenberg form

$$H_{S=1/2} = -\frac{3}{8}\,t - \frac{1}{2}\,t \sum_{<i,j>} \mathbf{S}_i \cdot \mathbf{S}_j \ . \tag{2.19}$$

In the general case, the double exchange Hamiltonian involves powers of the scalar product $(\mathbf{S}_i \cdot \mathbf{S}_j)^n$ up to $n = 2S$.

3. Numeric representation

There are four prerequisites a basis set should fulfill:

- It must be rapidly generated
- matrix elements are easy to compute
- modest need of memory
- fast access of states.

We will discuss the best basis sets and there numerical representation for spin and charge systems separately.

3.1 Spin-1/2 systems

Instead of the two spin values ± 1 we use the integers $n_i = \frac{\sigma_i + 1}{2} \in \{0, 1\}$. One is prompted to identify the sequence of n_i values as bit-pattern of the integer $I = \sum_{l=1}^{N} n_l \, 2^{l-1}$. For instance the basis state $|\psi\rangle = |-1, +1, -1, +1\rangle$ is represented by $n = \{0101\}$, which again is mapped onto the integer 4. This representation has two advantages, it keep the memory requirements as small as possible and it speeds up certain numerical operations.

Since $S^z = \sum_{i=1}^{N} S_i^z$ commutes with the Hamiltonian, the Hamilton matrix is block-diagonal in the sectors with fixed S^z values, i.e. fixed numbers N^σ of σ-spins. For a given S^z-sector the number of ones in the bit-pattern is fixed, which reduces the number of basis states to

$$L = \binom{N}{N\uparrow} , \tag{3.1}$$

where N is the number of lattices sites and

$$S^z = \frac{1}{2} \, 2N^\uparrow - N \, .$$

For instance, if the number of sites is $N = 16$ there are $2^{16} = 65536$ possible basis states in total, whereas there are merely $\binom{16}{8} = 12870$ for $S^z = 0$, i.e. $N^\uparrow = N^\downarrow = 8$, which is much less. Translation and Rotation could also be exploited which would reduce the number of basis state even further.

3.1.1 Generation of basis states

Not all integer values represent a permissible configuration, since the number of ones and zeros in the bit-pattern are fixed. We generate the basis states in such a way that the corresponding integer values are in increasing order. The basis states and there integer representations are therefore

$$
\begin{aligned}
|\varphi_1\rangle &= \{\overbrace{0,0,\ldots,0,0}^{N-N^\uparrow},\overbrace{1,1,1,\ldots,1}^{N^\sigma}\}; & I_1 &= 2^{N^\sigma}-1\\
|\varphi_2\rangle &= \{0,0,\ldots,0,1,0,1,1,\ldots,1\}; & I_2 &= 2^{N^\uparrow+1}-1-2^{N^\uparrow-1}\\
|\varphi_3\rangle &= \{0,0,\ldots,0,1,1,0,1,\ldots,1\}; & I_3 &= 2^{N^\uparrow+1}-1-2^{N^\uparrow-2}\\
&\vdots \qquad \vdots\\
|\varphi_L\rangle &= \{\underbrace{1,1,1,\ldots,1}_{N^\uparrow},\underbrace{0,0,\ldots,0,0}_{N-N^\uparrow}\}; & I_L &= 2^N-2^{N-N^\uparrow}\ .
\end{aligned}
$$

As an example we consider a four-site cluster with $S^z = 0$, i.e. two up and two down spins. Since the basis states are ordered, basis states given in the

no	1	2	3	4	5	6
bit	0011	0101	0100	1001	1010	1100
integer	3	5	6	9	10	12

Table 3.1. *Example for the representation of spin pattern as integers.*

spin representation can be rapidly by bisection search.

3.2 Electronic systems

For the electronic systems described above, i.e. Hubbard, Anderson, Emery and t-J, we can construct a convenient basis in real space. Here we restrict the discussion to a single orbital per lattice site. A generalization is obvious. The vector in real space can be written as

$$
|\psi\rangle = \prod_{i=1}^{N\uparrow} a^+_{\Gamma_i^\uparrow} \prod_{j=1}^{N\downarrow} a^+_{\Gamma_j^\downarrow} |0\rangle \tag{3.2}
$$

where $|0\rangle$ denotes the vacuum state and $\Gamma_i^\uparrow$ is the lattice site of the i-th spin-up electron and $\Gamma_j^\downarrow$ is the lattice site of the j-th spin-down electron. For instance

$$\left| \begin{matrix} 1 & 2 & 3 & 4 \\ \uparrow & \sqcup & \downarrow & \uparrow\downarrow \end{matrix} \right\rangle \tag{3.3}$$

is represented by $\Gamma^{\uparrow} = \{1, 4\}$ and $\Gamma^{\downarrow} = \{3, 4\}$. Another way to represent this basis is by

$$|\psi\rangle = \prod_{i=1}^{N} (a_{i\uparrow}^{+})^{n_i^{\uparrow}} \prod_{i=1}^{N} (a_{j\downarrow}^{+})^{n_j^{\downarrow}} \; |0\rangle \tag{3.4}$$

where $n_i^{\uparrow}, n_j^{\downarrow} \in \{0, 1\}$ indicate whether or not site i is occupied by a spin-up or spin-down electron. The state (3.3) is represented by $n^{\uparrow} = \{1, 0, 0, 1\}$ and $n^{\downarrow} = \{0, 0, 1, 1\}$. N is the number of lattice sites. Yet another way to encode the same basis is

$$|\psi\rangle = \prod_{i=0}^{N} O_i \, |0\rangle \qquad O_i \in \{\hat{1},\ a_{i\uparrow}^{+},\ a_{i\downarrow}^{+},\ a_{i\uparrow}^{+}\, a_{i\downarrow}^{+}\} \ , \tag{3.5}$$

where the Operator O_i creates either an empty site, a site occupied by an up- or down-electron, or a doubly occupied site. The number of basis states is 4^N. Doubly occupied site are forbidden in the tJ model and the number of basis-states reduces in this case to 3^N. Since the electronic spin is conserve, $N_{\uparrow}$ and $N_{\downarrow}$ are good quantum numbers. The number of basis states in the sector of fixed N_{σ} values is therefore

$$\binom{N}{N_{\uparrow}} \binom{N}{N_{\downarrow}}$$

As an example take $N = 16$ and $N_{\uparrow} = N_{\downarrow} = 8$. The number of basis states is then $4^{16} = 4.294.967.296$, whereas $\binom{16}{8}\binom{16}{8} = 165.636.900$ In the t-J-model there is the additional constraint that there must not be any double-occupancy. The number of basis states reduces further to

$$\frac{N!}{N_{\downarrow}! N_{\uparrow}! N_h!} \ ,$$

where $N_h = N - N_{\downarrow} - N_{\uparrow}$ is the number of holes, or rather the number of empty sites. We implicitly assume that there are less electrons than sites, i.e. we are below half-filling. In the just mentioned half filling example the number of states is merely 12870. In all models, given the proper boundary conditions, translational invariance can be exploited which allows to reduce the number of basis states roughly by a factor N.

For the same reasons as before it is recommended to compress the representation. To this end representation (3.4) is favorable, since the two spin species are separately treated and for each spin-direction the sequence of values n_i^{σ} can be interpreted as a bit-pattern. In the previous example $n^{\uparrow} = \{1, 0, 0, 1\}$ corresponds to the integer $I^{\uparrow} = 9$ and $n^{\downarrow} = \{0, 0, 1, 1\}$ corresponds to $I^{\uparrow} = 3$. Each basis-state is therefore represented by a pair of integers $(I^{\uparrow}, I^{\downarrow})$.

3.2.1 Generation of basis states

The generation if the basis states is similar to that for the spin systems. The only difference is that we have to generate two integers fort the two spin species. For spin-σ there are

$$L^\sigma = \binom{N}{N^\sigma}$$

basis states. The total number of states for a given sector $N^\uparrow, N^\downarrow$ is $L = L^\uparrow L^\downarrow$.

3.3 Computation of the Hamilton matrix

Here we want to compute the matrix elements

$$h_{\nu'\nu} = \langle \Phi_{\nu'} | H | \Phi_\nu \rangle \tag{3.6}$$

of the Hamiltonian in suitable basis states $|\Phi_\nu\rangle$. To this end we split the Hamiltonian into individual contributions $H^{(l)}$

$$H = \sum_l H^{(l)} \tag{3.7}$$

such that the application of one such term $H^{(l)}$ to a basis state $|\Phi_\nu\rangle$ yields again a basis state or the null vector, i.e.

$$H^{(l)} |\Phi_\nu\rangle = h^{(l)}_{\nu'\nu} |\Phi_{\nu'}\rangle \, .$$

The full matrix element $\langle \Phi_{\nu'} | H | \Phi_\nu \rangle$ is obtained by summing up all contributions $h^{(l)}_{\nu'\nu}$. If there is only one term $H(l)$ in Hamiltonian that mediates between the two basis states $|\Phi_\nu\rangle$ and $|\Phi_{\nu'}\rangle$ than $h_{\nu'\nu} = h^{(l)}_{\nu'\nu}$.

For concreteness we consider the Hubbard Hamilton matrix in the real-space basis (3.4), characterized by the set of occupation numbers $|\Phi_\nu\rangle = \left|\{n^{(\nu)}_{i,\sigma}\}\right\rangle$ for all lattice sites i and the two spin directions, with $n^{(\nu)}_{i\sigma} \in \{0, 1\}$. The Hubbard interaction H_1 in (2.1) is diagonal in this basis, so we have

$$h_{\nu\nu} = U \sum_i n^{(\nu)}_{i\uparrow} n^{(\nu)}_{i\downarrow} \, .$$

There are no other contributions to the diagonal elements. Each summand in the kinetic energy of (2.1) represents an individual contribution to (3.7). It is, however, more sensible to combine the back-and-forth hopping processes for a particular nearest-neighbour pair

$$H^{(l)} = -t \left(a^\dagger_{i_0\sigma_0} a_{j_0\sigma_0} + h.c. \right) \, . \tag{3.8}$$

Application of one of these terms, $H^{(l)}$ say, to a basis state $|\Phi_\nu\rangle = \big|\{n^{(\nu)}_{i,\sigma}\}\big\rangle$ results either in the null vector, if $n^{(\nu)}_{i_0\sigma_0}$ and ${}^{(\nu)}n_{j_0\sigma_0}$ are both occupied or empty, i.e.

$$c_l = 0\ ; \qquad \text{if } n^{(\nu)}_{i_0,\sigma_0} = n^{(\nu)}_{j_0,\sigma_0}\ .$$

Otherwise, the hopping process is possible and results in another basis state $|\Phi_{\nu'}\rangle = \big|\{n^{(\nu')}_{i,\sigma}\}\big\rangle$ which differs from $|\Phi_\nu\rangle$ only in the exchange of the occupation number $n^{(\nu)}_{i_0,\sigma_0}$ and $n^{(\nu)}_{j_0,\sigma_0}$, i.e.

$$n^{(\nu')}_{i,-\sigma_0} = n^{(\nu)}_{i,-\sigma_0} \qquad \forall i$$

$$\begin{aligned} n^{(\nu')}_{i,\sigma_0} &= n^{(\nu)}_{i,\sigma_0} \qquad \forall i \neq i_0, j_0 \\ n^{(\nu')}_{i_0,\sigma_0} &= n^{(\nu)}_{j_0,\sigma_0} \\ n^{(\nu')}_{j_0,\sigma_0} &= n^{(\nu)}_{i_0,\sigma_0}\ . \end{aligned} \tag{3.9}$$

There is only one hopping process $H^{(l)}$ mediating between the two basis states under consideration. The respective matrix element is therefor

$$h_{\nu'\nu} = \begin{cases} -t\ S & \text{if (3.9) is fulfilled,} \\ 0 & \text{otherwise.} \end{cases} \tag{3.10}$$

The hopping process can result in a sign S due to the fermi statistics of the electrons. E.g. consider a two-dimensional 4×4 lattice. The lattice sites are enumerated e.g. as follows

$$\begin{array}{cccc} 1 & 2 & 3 & 4 \\ 5 & 6 & 7 & 8 \\ 9 & 10 & 11 & 12 \\ 13 & 14 & 15 & 16 \end{array}\ .$$

There are many other ways of numbering the sites. The choice is arbitrary but fixed for the entire calculation. We consider the hopping between the adjacent sites 2 and 6 of one spin species. In the following we suppress the spin indices. The state $|\Phi_\nu\rangle$ be given by $\{n_{i\sigma}\} = \{0,0,1,1,\ 1,1,0,0,\ 0,0,0,0,\ 0,0,0,0\}$. The state reads according to (3.4)

$$|\Phi_\nu\rangle = a_3^\dagger a_4^\dagger a_5^\dagger a_6^\dagger |0\rangle\ .$$

Application of the hopping operator

$$-t(a_2^\dagger a_6 + a_6^\dagger a_2)$$

results in the state

$$|\Phi_\nu\rangle = a_3^\dagger a_4^\dagger a_5^\dagger a_2^\dagger \,|0\rangle = -\, a_2^\dagger a_3^\dagger a_4^\dagger a_5^\dagger \,|0\rangle \ .$$

The sign is given by

$$S = (-1)^{\Delta n} \ ,$$

where Δn is the number of electrons at the lattice sites between the sites i and j. In the above example $\Delta n = 3$.

What have we learned so far. We started out with an index $\nu \in \{1, \ldots, L\}$ for one of the basis states $|\Phi_\nu\rangle$, for which we know the representation $\{n_{i\sigma}^{(\nu)}\}$. The individual terms of the Hamiltonian couple to other basis states represented by a bit-pattern $\{n'_{i\sigma}\}$ or rather the corresponding integer representations $(I'_\uparrow, I'_\downarrow)$. We still need to know the corresponding index ν' of the basis state. Here it comes in handy that the basis states have been generated with increasing integer representation, so we can invoke a bisection search to find the respective indices ν. From the point of view of computer time this is crucial. The number of basis states one is interested in is typically $L = 10^8$ and more. A brute force search takes $O(L)$ steps, while the bisection search merely needs $O(\log_2(L))$ operations. For 10^8 the difference is a factor of 10^6. The index search has to be performed for each nonzero matrix element of the hamiltonian. In the Hubbard model there are roughly

$$N_{\mathrm{nz}} = L\ d\ N \ , \tag{3.11}$$

where d is the dimension of the underlying lattice and N the number of lattice sites.

The sign depends on the order in which electrons appear after the hopping process. For the interaction part, th prefactor is either U

3.4 Sparse matrices

In the above-mentioned representation the many-body Hamilton-matrices H_{ij} are sparse. We have seen that only a small fraction of all matrix elements is not zero. It is sensible to store only the nonzero matrix elements not only to save memory but also to speed up operations of the form $H\boldsymbol{x}$ which form the heart of the exact diagonalization schemes that will be discussed in the next chapter. The most transparent algorithm to store sparse matrices is

Algorithm 3.4.1: COMPACT STORAGE$(H, H_c, ind, N_{\mathrm{nz}})$

$$\textbf{initialize:} \begin{cases} L &= \mathrm{size}(H) \\ N_{\mathrm{nz}} &= 0 \end{cases}$$

$$\textbf{for } i = 1 \textbf{ to } L$$
$$\begin{cases} \textbf{for } j = 1 \textbf{ to } L \\ \quad \begin{cases} \textbf{if } H(i,j) \neq 0 \\ \quad \textbf{then} \begin{cases} N_{\mathrm{nz}} &= N_{\mathrm{nz}} + 1 \\ H_c(k) &= H(i,j) \\ ind(k,1) &= i \\ ind(k,2) &= j \end{cases} \end{cases} \end{cases}$$

The only operation the matrix will be used for is action on a vector. The compact storage can directly be used to perform only the nonzero multiplications as depicted in the following algorithm

Algorithm 3.4.2: MULTIPLY H $\boldsymbol{x}(H_c, ind, N_{\mathrm{nz}}, \boldsymbol{x}, \boldsymbol{y})$

$$\textbf{initialize:} \left\{ \boldsymbol{y} = 0 \right.$$

$$\textbf{for } i = 1 \textbf{ to } N_{\mathrm{nz}}$$
$$\begin{cases} i_1 &= \mathrm{ind}(i,1) \\ i_2 &= \mathrm{ind}(i,2) \\ y(i_1) &= y(i_1) + t(i) * x(i_2) \end{cases}$$

4. Exact diagonalization

In this chapter we describe methods for the exact evaluation of eigenvalues and eigenvectors of many-body Hamiltonians. There are very powerful exact diagonalization algorithms in the textbooks about numerical mathematics. A severe drawback of these schemes is there limitation to matrix sizes of the order $N = O(10^3)$. Strongly correlated many-body problems, however, start with $N = O(10^8)$ and go way beyond. It is obvious that conventional schemes are powerless in these cases. On the other hand there are no better algorithms for the full diagonalize of general hermitean matrices. The loop holes are the words 'full diagonalization' and 'general'. The interesting quantum features of strongly correlated many-body systems show up at very low temperatures. For the theoretical description of these temperatures, merely the groundstate and a few low-laying eigenvalues and the corresponding eigenvectors are required. Moreover, for most systems an appropriate basis can be found, in which the Hamilton-matrices are sparse. The number of nonzero matrix elements is typically $O(N)$ rather than $O(N^2)$.

A standard scheme from numerical mathematics, which allows to take advantage of the sparseness of a matrix and which allows to concentrate on the groundstate only, is the so-called power method or rather the vector-iteration due to von Mises.

4.1 The Power Method

The Power method is a simple and yet powerful technique to determine the eigenvector corresponding to the 'dominant' eigenvalue. The eigenvalue problem for the Hamilton operator H under consideration reads

$$\hat{H}\,|\varphi_l\rangle = \epsilon_l\,|\varphi_l\rangle \qquad \text{with} \quad \langle\varphi_l\,|\varphi_{l'}\rangle = \delta_{l,l'} \tag{4.1}$$

with real eigenvalue ε_l and mutually orthogonal and normalized eigenvectors $|\varphi_l\rangle$. The eigenvalues may be degenerate. We introduce a spectral shift

$$\hat{H} \to \hat{H}' = \hat{H} - E_s\hat{I} \qquad \text{and} \qquad \epsilon_l \to \epsilon_l' = \epsilon_l - E_s\ ,$$

which does not affect the eigenvectors $|\varphi_l\rangle$. Therefore, we can adapt E_s in such a way that the ground state yields the dominant eigenvalue, i.e.

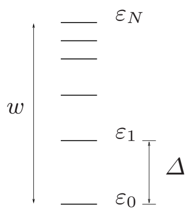

Fig. 4.1. Schematic representation of the eigenvalues of the Hamiltonian. The gap between the lowest two eigenvalues is denoted by Δ

$$|\epsilon'_0| \geq |\epsilon'_l| \quad \forall \, l \, .$$

To ensure that the groundstate energy ϵ'_0 has the greatest modulus of all eigenvalues the condition

$$\epsilon'_0 < -\frac{W}{2} = \frac{\epsilon_N - \epsilon_0}{2}$$

has to be fulfilled, which yields the condition

$$E_s > \frac{\epsilon_0 + \epsilon_N}{2} \, .$$

Next we want to apply the Power method to $\hat{H}'$ starting with an initial vector $|x_0\rangle$ chosen at random, possibly subject to suitable symmetry constraints. After n repeated applications of $\hat{H}'$ we obtain

$$|\tilde{x}_n\rangle \stackrel{\text{def}}{=} \hat{H}'^{\,n} \, |x_0\rangle = \sum_{l=0}^{N} |\varphi_l\rangle \epsilon'^{\,n}_l \underbrace{\langle \varphi_l \, | x_0 \, \rangle}_{c_l} \, , \tag{4.2}$$

where we have inserted an expansion of the initial state $|x_0\rangle$ in the basis of eigenstates $\{|\varphi_l\rangle\}$ with the coefficients c_l. The normalization yields

$$|x_n\rangle \stackrel{\text{def}}{=} \frac{|\tilde{x}_n\rangle}{||\tilde{x}_n||} = \frac{\sum_l c_l \epsilon'^{\,n}_l |\varphi_l\rangle}{\left(\sum_l |c_l|^2 \epsilon'^{\,2n}_l\right)^{1/2}} \, , \tag{4.3}$$

or, equivalently, by dividing numerator and denominator by $c_0 \, \epsilon'^{n}_0$

$$|x_n\rangle = \frac{\sum_l \frac{c_l}{c_0} \left(\frac{\epsilon'_l}{\epsilon'_0}\right)^n |\varphi_l\rangle}{\left(\sum_l \left(\frac{c_l}{c_0}\right)^2 \left(\frac{\epsilon'_l}{\epsilon'_0}\right)^{2n}\right)^{1/2}} \, . \tag{4.4}$$

We introduce the definition

$$q \stackrel{\text{def}}{=} \max_i \left| \frac{\varepsilon'_i}{\varepsilon'_0} \right| \, .$$

For the time being we assume that the groundstate energy is not degenerate and the initial vector has a non-vanishing overlap with the sought-for groundstate. In this case $q < 1$ and the Power method converges to the true groundstate

$$|x_n\rangle = |\varphi_0\rangle + O\left(q^n\right) \underset{n\to\infty}{\longrightarrow} |\varphi_0\rangle \ .$$

If the initial vector is orthogonal to the groundstate, the iteration converges to the lowest eigenstate which has a non-vanishing contribution in $|x_0\rangle$. This can be used directly to determine states with given symmetry, e.g. the dispersion relation of the lowest excitations. In order to guarantee the convergence towards the lowest energy for a given symmetry, one can choose an appropriate initial vector by imposing the desired symmetry on a random vector. The ratio q is either $\left|\frac{\varepsilon'_1}{\varepsilon'_0}\right|$ or $\left|\frac{\varepsilon'_N}{\varepsilon'_0}\right|$. The best convergence is achieved if

$$\left|\frac{\varepsilon'_1}{\varepsilon'_0}\right| = \left|\frac{\varepsilon'_N}{\varepsilon'_0}\right| \quad \Rightarrow q = \left|\frac{1-\Delta/W}{1+\Delta/W}\right| \ .$$

Obviously, the convergence is governed by the ratio Δ/W. The closer the excited states is to the groundstate, the longer it takes to get rid of its contribution in $|x_n\rangle$. If the lowest eigenvalue is degenerate

$$\varepsilon'_0 = \varepsilon'_1 = \ldots = \varepsilon'_L \ < \ \varepsilon_{L+1}$$

then then the Power iterates $|x_n\rangle$ converge towards the projection of the initial vector $|x_0\rangle$ onto the eigenspace of the first eigenvalue:

$$|x_n\rangle \ \underset{n\to\infty}{\longrightarrow} \ \frac{\mathbb{P}\,|x_0\rangle}{\langle x_0|\mathbb{P}\,|x_0\rangle}$$

where $\mathbb{P}$ is the projector onto the eigenspace of the ground state

$$\mathbb{P} = \sum_{l=0}^{L} |\varphi_l\rangle\langle\varphi_l| \ .$$

Using the expansion (4.2) for the energy-expectation value

$$\langle x_n|\hat{H}|x_n\rangle = \epsilon_0 + O\left(\left|\epsilon_1/\epsilon_0\right|^{2n}\right)$$

shows that the energy converges faster than the vector $|x_n\rangle$. On passing we note that the power-method allows also to determine excited states. Once the ground state is approximately determined a new sequence of iterations is started with an initial vector orthogonal to the approximate groundstate. Since the groundstate is approximate and due to the presence of numerical noise, the vectors $\boldsymbol{x_n}$ loose the orthogonality to the ground with increasing number of iterations and it is expedient to re-orthogonalize the vectors once in a while.

4.1.1 Eigenvalue Estimates

For the power method as well as for other numerical algorithms discussed in succeeding chapters it is advantageous to have a rough idea about the eigenvalue spectrum or to be able to give exact bounds for the individual eigenvalues.

Theorem of Geršgorin. We start out with the theorem of Geršgorin in its most elementary form. For the proof or generalizations we refer the reader to standard textbooks on numerical mathematics. The theorem states: In every disc in the complex plane centered at $z = H_{jj} + i * 0$ with radius $R_j = \sum_{l \neq j} |H_{lj}|$ there is at least one eigenvalue of $\hat{H}$. For a hermitean matrix $\hat{H}$ all eigenvalues are, of course, real. Consider, for example an example, the tight-binding matrix

$$
H = \begin{pmatrix}
0\,1\,0\,.\,.\,.\,1 \\
1\,0\,1\,0\,.\,.\,. \\
0\,1\,0\,1\,0\,.\,. \\
.\,0\,1\,0\,1\,.\,. \\
.\,.\,0\,1\,0\,.\,. \\
.\,.\,.\,.\,.\,.\,. \\
1\,.\,.\,.\,.\,.\,.
\end{pmatrix}
$$

According to the theorem of Geršgorin all eigenvalues ε_i are located in the interval $-2 \leq \varepsilon_i \leq 2$, which is in agreement with the exact result $\varepsilon = 2\cos(\frac{2\pi n}{N})$, where N is the dimension of the matrix and n takes on integer values between 0 and $N-1$.

Trace of powers of *H*. It is sometimes convenient to exploit the trace of $\hat{H}^\nu$ for integer powers ν. The spectral theorem for hermitean matrices reads

$$
H = UDU^T
$$

with D being the diagonal matrix of the eigenvalues of H. and the j-th column of the unitary matrix U contains the j-the eigenvector corresponding to the eigenvalue $\epsilon_j = d_{jj}$. The invariance of the trace against cyclic permutation yields

$$
\mathrm{tr}(H^\nu) = \mathrm{tr}(UD^\nu U^T) = \mathrm{tr}(D^\nu) = \sum_j \epsilon_j^\nu \,.
$$

For the two lowest powers the result is particularly simple

$$
\begin{aligned}
\sum_i \varepsilon_i &= \mathrm{tr}\,\hat{H} = \sum_i H_{ii} \\
\sum_i \varepsilon_i^2 &= \sum_{i,j} |H_{ij}|^2 \,.
\end{aligned}
$$

In the theory of superconductivity the matrix

$$H = \begin{pmatrix} 1 & 1 & 1 & \cdots \\ 1 & 1 & 1 & \cdots \\ 1 & 1 & 1 & \cdots \\ \vdots & \vdots & \vdots & \ddots \end{pmatrix}$$

is of some importance[**?**]. The powers of H obey the relation $H^\nu = N^{\nu-1}H$ which leads along with $\mathrm{tr}(H^\nu) = N^\nu$ to the result

$$\sum_j \epsilon_j^\nu = N^\nu \quad ; \qquad \text{for } \nu = 1, 2, \dots \ ,$$

which implies

$$\varepsilon_1 = N \text{ and } \varepsilon_i = 0 \quad \forall i \neq N \ .$$

In this particular example we are able to infer the entire spectrum from the powers of H. Needless to say, that this is an extremely lucky exception. Finally, we want to apply the theorem of Geršgorin to this particular example. The result, which is readily obtained, reads

$$2 - N \ \leq \ \varepsilon_i \ \leq \ N \ .$$

It is obviously correct but not very useful for $N \gg 1$.

Exact interval bounds. We will now derive a very useful exact expression for lower and upper bounds of individual eigenvalues. We assume that we have a reasonable approximation $|\psi\rangle$ for an normalized eigenvector, obtained e.g. by the Power method or Quantum Monte Carlo techniques. The corresponding approximate energy reads $\varepsilon = \langle\psi|H|\psi\rangle$. In addition we define the standard deviation $\sigma = \sqrt{< H^2 > - < H >^2}$. We will prove that there is at least one exact eigenvalue of $\hat{H}$ in the interval

$$I = [\varepsilon - \sigma, \varepsilon + \sigma] \ .$$

First, we expand the vector $|\psi\rangle$ in the basis $\{|\varphi_i\rangle\}$ of eigenvectors of $\hat{H}$

$$|\psi\rangle = \sum_i c_i \, |\varphi_i\rangle \ .$$

The variance can then be estimated by

$$\sigma^2 = \sum_i |c_i|^2 \, (\varepsilon_i - \varepsilon)^2 \geq (\varepsilon_m - \varepsilon)^2 \underbrace{\sum_i |c_i|^2}_{=1} \ ,$$

where ε_m denotes the exact eigenvalue that is closest to ε. We infer that $|\varepsilon_m - \varepsilon| \leq \rho$ and hence

$$\varepsilon_m \in [\varepsilon - \sigma, \varepsilon + \sigma] \; .$$

Different to the meaning of standard deviations in statistics, in the present context, the exact eigenvalue lies with certainty in the one-sigma regime. The standard-deviation can be used as convergence criterion for Quantum-Monte Carlo simulations or exact diagonalization techniques.

WVL: vom anfang bis hier am 29.10. ueberarbeitet

4.2 The Lanczos Method

The Power method uses only a small part of the information actually provided by the power method. One can do much better with only a little more computational effort. This goal is achieved by the Lanczos method.

4.2.1 The poor man's Lanczos scheme

To begin with, we analyze the information content of the first Power method iteration. After one step we have two normalized vectors $|x_0\rangle$ and $|x_1\rangle$, which are in general not orthogonal, and the corresponding energy-expectation values are

$$E_0^P = \langle x_0|\hat{H}|x_0\rangle$$
$$E_1^P = \langle x_1|\hat{H}|x_1\rangle \; .$$

The basic idea of the Lanczos method is to diagonalize the Hamiltonian in the subspace spanned by $\{|x_0\rangle, |x_1\rangle\}$, i.e. to minimize the energy of the variational Ansatz

$$\left|x_1^L\right\rangle = \alpha\,|x_0\rangle + \beta\,|x_1\rangle$$
$$E_1^L = \min_{\alpha,\beta} \frac{\left\langle x_1^L\middle|H\middle|x_1^L\right\rangle}{\left\langle x_1^L\middle|x_1^L\right\rangle} \leq \langle x_1|H|x_1\rangle \; .$$

The last inequality follows since $\langle x_1|H|x_1\rangle$ corresponds to the special case $\alpha = 0, \beta = 1$. It can easily be shown that the energy of the Lanczos method is actually lower than that of the Power method provided $\langle x_1|\hat{H}|x_0\rangle \neq 0$.

This procedure can be repeated by choosing the Lanczos vector x_1^L as initial vector of the subsequent iteration. The results of the Power method are compared with those of the simple Lanzcos scheme for a 10×10 tight binding matrix.

$$H = \begin{pmatrix} -1 & 1 & 0 & . & . \\ 1 & -1 & 1 & 0 & . \\ . & 1 & -1 & 1 & 0 \\ . & . & 1 & -1 & 1 \\ . & . & . & 1 & \ddots \end{pmatrix}$$

where an appropriate spectral shift has been introduce. The energies are depicted in Fig. 4.2. Obviously, the 'poor man's lanczos' scheme is superior,

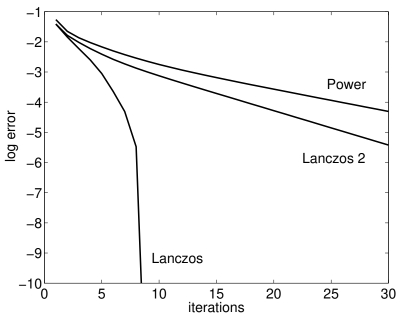

Fig. 4.2. Comparison of the speed of convergence to the exact ground-state energy of the Power method and the Lanczos method. Lanzcos 2 stands for the introductory example of only two vectors

but not overwhelmingly so. Particularly disturbing is the observation, that it takes more than 10 iterations, which is the dimension of the matrix, to achieve convergence.

It is, however, straight forward, to generalized and improve the above ideas. Instead of taking only two vectors into account, we keep all vectors $|x_n\rangle$, generated during the iterations of the Power method. The set of vectors $|x_n\rangle$ spans the n-dimensional Krylov space. The minimization of the variational energy leads to the generalized eigenvalue problem depending on the matrix elements of the Hamiltonian and on the overlap matrix of the vectors $|x_n\rangle$. Linear dependencies of these basis states can lead to severe numerical problems. It is therefore better to transform the basis set $\{|x_n\rangle\}$ into an orthonormal set of vectors that still spans the Krylov space.

4.2.2 Lanczos Method for Hermitean Matrices

The Lanczos procedure starts with an appropriate normalized initial vector $|x_0\rangle$, chosen along the lines outlined before. The corresponding energy-expectation value is

$$\varepsilon_0 = \langle x_0|\hat{H}|x_0\rangle \, .$$

Next we apply the Hamiltonian to $|x_0\rangle$ in order to determine the next basis vector

$$|\tilde{x}_1\rangle = \hat{H}|x_0\rangle - \varepsilon_0 \, |x_0\rangle \, .$$

Apparently, the two vectors are orthogonal.

$$\langle x_0 \,|\tilde{x}_1 \,\rangle = 0$$

Again, the vector is normalized

$$|x_1\rangle = \frac{|\tilde{x}_1\rangle}{||\tilde{x}_1||}$$

and the energy-expectation value is computed

$$\varepsilon_1 = \langle x_1|\hat{H}|x_1\rangle \,.$$

The next basis vector is generated using the prescription

$$|\tilde{x}_2\rangle = H|x_1\rangle - \varepsilon_1\,|x_1\rangle - k_1|x_0\rangle$$

We choose the coefficients ε_2 and k_1 such that $|\tilde{x}_2\rangle$ is orthogonal to the previous basis vectors $\{|x_0\rangle, |x_1\rangle\}$:

$$\langle x_1 \,|\tilde{x}_2 \,\rangle = \langle x_1|\hat{H}|x_1\rangle - \varepsilon_1 - k_1 \underbrace{\langle x_1 \,|x_0 \,\rangle}_{=0} = 0$$

$$\langle x_0 \,|\tilde{x}_2 \,\rangle = \langle x_0|\hat{H}|x_1\rangle - \varepsilon_1 \underbrace{\langle x_0 \,|x_1 \,\rangle}_{=0} - k_1 = 0$$

Hence, ε_1 has again the interpretation of an expectation value,

$$\varepsilon_1 = \langle x_1|\hat{H}|x_1\rangle \;\text{ and }\; k_1 = \langle x_0|\hat{H}|x_1\rangle \,.$$

By construction, the quantity k_1 is real, since

$$k_1^* = \langle x_1|\hat{H}|x_0\rangle = \langle x_1 \,|\tilde{x}_1 \,\rangle + \varepsilon_0 \underbrace{\langle x_1 \,|x_0 \,\rangle}_{=0} = ||\tilde{x}_1|| \in \mathbb{R} \,.$$

We add the normalized vector $|\tilde{x}_2\rangle$ to the set of orthonormal basis states $\{|x_0\rangle, |x_1\rangle, |x_2\rangle\}$. Next we skip a several iterations steps and assume that we have already generated a set of n mutually orthonormal vectors $\{|x_0\rangle, |x_1\rangle, \ldots |x_n\rangle\}$. The next vector $|x_{n+1}\rangle$ is determined as follows

$$\begin{aligned}
|\tilde{x}_{n+1}\rangle &= \hat{H}|x_n\rangle - \varepsilon_n\,|x_n\rangle - k_n\,|x_{n-1}\rangle \\
\varepsilon_n &= \langle x_n|\hat{H}|x_n\rangle \\
k_n &= \langle x_{n-1}|\hat{H}|x_n\rangle = ||\tilde{x}_n|| \\
|x_{n+1}\rangle &= \frac{|\tilde{x}_{n+1}\rangle}{||\tilde{x}_{n+1}||} \,.
\end{aligned}$$

We prove that $|x_{n+1}\rangle$ is orthogonal to all previous vectors.

$$\langle x_n \,|\tilde{x}_{n+1} \,\rangle = \underbrace{\langle x_n|\hat{H}|x_n\rangle}_{\varepsilon_n} - \varepsilon_n \underbrace{\langle x_n \,|x_n \,\rangle}_{=1} - k_n \underbrace{\langle x_n \,|x_{n-1} \,\rangle}_{=0} = 0$$

$$\langle x_{n-1} \,|\tilde{x}_{n+1} \,\rangle = \underbrace{\langle x_{n-1}|\hat{H}|x_n\rangle}_{k_n} - \varepsilon_n \underbrace{\langle x_{n-1} \,|x_n \,\rangle}_{=0} - k_n \underbrace{\langle x_{n-1} \,|x_{n-1} \,\rangle}_{=1} = 0$$

For $i = 1, \ldots, n-2$ we have

$$\langle x_i \,|\tilde{x}_{n+1}\,\rangle = \langle x_i|\hat{H}|x_n\rangle - \varepsilon_n \underbrace{\langle x_i\,|x_n\,\rangle}_{=0} - k_n \underbrace{\langle x_i\,|x_{n-1}\,\rangle}_{=0} = \langle x_i|\hat{H}|x_n\rangle \;.$$

The hermitecity of $\hat{H}$ yields

$$\begin{aligned}
\langle x_i|\hat{H}|x_n\rangle &= \Big(\langle x_n|\hat{H}|x_i\rangle\Big)^* \\
&= \Big(\langle x_n|(|\tilde{x}_{i+1}\rangle + \varepsilon_i\,|x_i\rangle + k_i\,|x_{i-1}\rangle)\Big)^* \\
&= \Big(\underbrace{\langle x_n\,|\tilde{x}_{i+1}\,\rangle}_{=0} + \varepsilon_i \underbrace{\langle x_n\,|x_i\,\rangle}_{=0} + k_i \underbrace{\langle x_n\,|x_{i-1}\,\rangle}_{=0}\Big)^* \\
&= 0 \;,
\end{aligned}$$

which shows that the constructed set of $n+1$ vectors is indeed orthogonal. Moreover, it shows that the Hamilton matrix is tridiagonal in the Lanczos basis:

$$H^t_{ij} = \begin{pmatrix} \varepsilon_0 & k_1 & 0 & . & . \\ k_1 & \varepsilon_1 & k_2 & 0 & . \\ 0 & k_2 & \varepsilon_2 & k_3 & 0 \\ . & 0 & k_3 & \varepsilon_3 & k_4 \\ . & . & 0 & k_4 & \varepsilon_4 \end{pmatrix} \qquad . \tag{4.5}$$

The remaining task is the solution of the eigenvalue problem of the tridiagonal matrix H^t

$$H^t \boldsymbol{c}^{\boldsymbol{\nu}} = E^\nu \; \boldsymbol{c}^{\boldsymbol{\nu}} \;.$$

The best approximation to the eigenvectors of the original Hamiltonian expanded in the truncated (Lanczos-) basis are therefore given by

$$|\psi^\nu\rangle = \sum_i \; c_i^\nu \; |x_i\rangle \;,$$

where the components c_i of the eigenvectors of the tridiagonal matrix H^t present the expansion coefficients in the Lanczos basis.

We summarize the Lanczos algorithm

Algorithm 4.2.1: LANCZOS ALGORITHM(.)

assign: $n_{\max}, N_{\text{diag}}, L, \delta$

$$\textbf{initialize:} \begin{cases} |\tilde{x}_0\rangle & : \text{ appropriate initial vector} \\ |x_{-1}\rangle & = 0 \\ n & = 0 \\ \textit{converged} & = \textbf{ false} \end{cases}$$

while not *converged*

$$\textbf{do} \begin{cases} k_n = \sqrt{\langle \tilde{x}_n | \tilde{x}_n \rangle} \\ \textbf{if } k_n < \delta \textbf{ then } \textit{converged} = \textbf{ true} \\ |x_n\rangle = |\tilde{x}_n\rangle / k_n \\ \varepsilon_n \quad = \langle x_n | \hat{H} | x_n \rangle \\ \textbf{if } \text{MOD}(n, N_{\text{diag}}) = 0 \\ \quad \textbf{then} \begin{cases} H_t = \text{TRIDIAGONALMATRIX}(\{\varepsilon_0, \ldots \varepsilon_n\}; \{k_1 \ldots k_n\}) \\ \text{SOLVE EIGENVALUE-PROBLEM}(H_t; E_\nu, \boldsymbol{c}_\nu) \\ \textbf{if } E_1 \ldots E_L \text{ are converged } \textbf{then } \textit{converged} = \textbf{ true} \end{cases} \\ |\tilde{x}_{n+1}\rangle \qquad\qquad = \hat{H}|x_n\rangle - \varepsilon_n |x_n\rangle - k_n |x_{n-1}\rangle \\ n \qquad\qquad = n + 1 \\ \textbf{if } n \geq n_{\max} \textbf{ then } \textit{converged} = \textbf{ true} \end{cases}$$

In Fig. 4.2 the general performance of the Lanczos method is compared with that of the Power method and that of the simple Lanczos scheme. We observe a much faster convergence of the results of the Lanczos method and, as expected, exact convergence is achieved after 10 steps.

4.2.3 Dynamical Correlations

Dynamical correlations describe how a crystal reacts to weak external perturbations denoted by $E(t)$. Linear response theory expresses the reaction as

$$R(t) = \int_{-\infty}^{t} \chi(t,t')\, E(t')\, dt' \tag{4.6}$$

where χ is actually a function of the time-differences

$$\chi(t,t') = \chi(t-t')\ . \tag{4.7}$$

The response (4.6) has the form of a convolution and Fourier transformation yields a simple product

$$R(\omega) = \chi(\omega) E(\omega)\ . \tag{4.8}$$

The dynamical correlation function $\chi(\omega)$, or rather *susceptibility*, for zero temperature can be computed by the Lanczos procedure with little extra effort.

4.2.4 Dynamic Green's functions

To every dynamical correlation function corresponds a Green's function. For an operator $\hat{O}$ the retarded Green's function is defined by

$$\begin{aligned}\left\langle\!\left\langle \hat{O}(t)\,;\hat{O}^{\dagger}\right\rangle\!\right\rangle &\overset{\text{def}}{=} -\mathrm{i}\,\Theta(t)\,\left\langle [\hat{O}(t),\hat{O}^{\dagger}]_{\varepsilon=\pm 1}\right\rangle \\ &= -\mathrm{i}\,\Theta(t)\,\left(\left\langle \hat{O}(t)\,\hat{O}^{\dagger}\right\rangle + -\varepsilon\left\langle \hat{O}^{\dagger}\,\hat{O}(t)\right\rangle\right)\ ,\end{aligned} \tag{4.9}$$

where in the second line the symbol $\langle\ \rangle$ denotes the thermodynamic average. Commutator ($\varepsilon = +1$) and anticommuator ($\varepsilon = -1$) Green's functions can be chosen at will. For a detailed introduction to the theory of Green's functions see e.g. [**?**]. At zero temperature, the average corresponds to the expectation value of the operators in the ground state $|\psi_0\rangle$ of the many-particle system. In this we focus on $T = 0$. Finite temperatures will be discussed later on.

We proceed by inserting the Heisenberg time evolution of the operator $\hat{O}$

$$\hat{O}(t) = \mathrm{e}^{\mathrm{i}\hat{H}t}\,\hat{O}\,\mathrm{e}^{-\mathrm{i}\hat{H}t}\,, \qquad \hat{O} \overset{\text{def}}{=} \hat{O}(t=0) \tag{4.10}$$

into (4.9). Since $|\psi_0\rangle$ is the exact ground-state with energy E_0 we have

$$\mathrm{e}^{-\mathrm{i}\hat{H}t}\,|\psi_0\rangle = \mathrm{e}^{-\mathrm{i}E_0 t}\,|\psi_0\rangle \quad \text{and} \quad \langle\psi_0|\,\mathrm{e}^{\mathrm{i}\hat{H}t} = \langle\psi_0|\,\mathrm{e}^{\mathrm{i}E_0 t}\ , \tag{4.11}$$

and with $w^{+} = w + \mathrm{i}\delta$, where δ is an infinitesimal positive quantity, we obtain

$$\left\langle\!\left\langle \hat{O};\hat{O}^\dagger\right\rangle\!\right\rangle_w \stackrel{\text{def}}{=} \int_{-\infty}^{\infty} \mathrm{e}^{\mathrm{i}w^+t}\left\langle\!\left\langle \hat{O}(t),\hat{O}^\dagger\right\rangle\!\right\rangle dt \tag{4.12}$$
$$= -\mathrm{i}\int_0^\infty \mathrm{e}^{\mathrm{i}w^+t}\left(\left\langle \mathrm{e}^{\mathrm{i}\hat{H}t}\hat{O}\mathrm{e}^{-\mathrm{i}\hat{H}t}\hat{O}^\dagger\right\rangle - \varepsilon\left\langle \hat{O}^\dagger\mathrm{e}^{\mathrm{i}\hat{H}t}\hat{O}\mathrm{e}^{-\mathrm{i}\hat{H}t}\right\rangle\right) dt$$
$$= -\mathrm{i}\int_0^\infty \mathrm{e}^{\mathrm{i}w^+t}\left(\left\langle \hat{O}\mathrm{e}^{-\mathrm{i}(\hat{H}-E_0)t}\hat{O}^\dagger\right\rangle - \varepsilon\left\langle \hat{O}^\dagger\mathrm{e}^{\mathrm{i}(\hat{H}-E_0)t}\hat{O}\right\rangle\right) dt$$
$$= -\mathrm{i}\left(\left\langle \hat{O}\int_0^\infty \mathrm{e}^{\mathrm{i}w^+t}\mathrm{e}^{-\mathrm{i}(\hat{H}-E_0)t}dt\,\hat{O}^\dagger\right\rangle - \varepsilon\left\langle \hat{O}^\dagger\int_0^\infty \mathrm{e}^{\mathrm{i}w^+t}\mathrm{e}^{\mathrm{i}(\hat{H}-E_0)t}dt\,\hat{O}\right\rangle\right).$$

With the aid of the spectral theorem the integral can now be evaluated. Now, taking into account the identity $-\mathrm{i}\,\mathrm{i} = 1$ and recalling that we perform the average in the ground state $|\psi_0\rangle$, we obtain

$$\begin{aligned}\left\langle\!\left\langle \hat{O},\hat{O}^\dagger\right\rangle\!\right\rangle_w =&\left\langle \hat{O}\frac{1}{w^+-(\hat{H}-E_0)}\hat{O}^\dagger\right\rangle - \varepsilon\left\langle \hat{O}^\dagger\frac{1}{w^++(\hat{H}-E_0)}\hat{O}\right\rangle\\ =&\langle\psi_0|\hat{O}\hat{O}^\dagger|\psi_0\rangle\left\langle\varphi_0\right|\frac{1}{w^+-(\hat{H}-E_0)}\left|\varphi_0\right\rangle\\ &-\varepsilon\,\langle\psi_0|\hat{O}^\dagger\hat{O}|\psi_0\rangle\left\langle\tilde{\varphi}_0\right|\frac{1}{w^++(\hat{H}-E_0)}\left|\tilde{\varphi}_0\right\rangle.\end{aligned} \tag{4.13}$$

The normalized state vectors $|\varphi_0\rangle$ and $|\tilde{\varphi}_0\rangle$, defined by,

$$|\varphi_0\rangle = \frac{\hat{O}^\dagger|\psi_0\rangle}{\sqrt{\langle\psi_0|\hat{O}\hat{O}^\dagger|\psi_0\rangle}} \qquad |\tilde{\varphi}_0\rangle = \frac{\hat{O}|\psi_0\rangle}{\sqrt{\langle\psi_0|\hat{O}^\dagger\hat{O}|\psi_0\rangle}} \tag{4.14}$$

are used as initial vectors for two independent Lanczos sequences. The tridiagonal form of $\hat{H}$, and likewise of the energy denominators $\tilde{H} = w\pm(H-E_0)$, in the Lanczos basis can be exploited to determine the expectation value of the inverse of $\tilde{H} = w\pm(H-E_0)$ in (4.14). As for the ground state we calculate the matrix elements for the Lanczos vectors

$$\begin{aligned}\langle\varphi_i|\hat{H}-E_0|\varphi_i\rangle &= \Delta\varepsilon_i\\ \langle\varphi_i|\hat{H}-E_0|\varphi_{i+1}\rangle &= k_i\\ \langle\varphi_i|\hat{H}-E_0|\varphi_j\rangle &= 0\,\forall_{i,j},|i-j|>1\end{aligned} \tag{4.15}$$

Along with the orthonormality

$$\langle\varphi_i\,|\varphi_j\,\rangle = \delta_{i,j}\ ,$$

we obtain the tridiagonal form

$$(w^+\pm(\hat{H}-E_0)) = \begin{pmatrix} w^+\pm\Delta\varepsilon_0 & k_1 & 0 & . & .\\ k_1 & w^+\pm\Delta\varepsilon_1 & k_2 & 0 & .\\ 0 & k_2 & w^+\pm\Delta\varepsilon_2 & k_2 & 0\\ . & 0 & k_3 & w^+\pm\Delta\varepsilon_3 & k_3\\ . & . & 0 & k_4 & \ddots \end{pmatrix}.$$

We need the $(0,0)$–element of the inverse. The (ij)-element of the inverse matrix can be expressed by

$$A^{-1}_{ij} = (-1)^{i+j}\,\frac{\det \Delta_{ij}}{\det A}\ ,$$

where Δ_{ij} denotes the submatrix of A obtained upon eliminating from A the i-th row and the j-th column. Especially for the sought-for $(0,0)$-element of the inverse is

$$A^{-1}_{00} = \frac{\det \Delta_{00}}{\det A}\ , \tag{4.16}$$

Because of the tridiagonal structure of the above matrix, the formula simplifies as follows. Consider the matrix

$$A = \begin{pmatrix} A_{00} & A_{01} & 0 & . & . \\ A_{10} & A_{11} & A_{12} & 0. & \\ 0 & A_{21} & A_{22} & A_{23} & 0 \\ . & 0 & A_{32} & A_{33} & A_{34} \\ . & . & 0 & A_{43} & A_{44} \end{pmatrix}$$

The determinant can be expanded along the first row and column yielding

$$\det(A) = A_{00} \det \begin{pmatrix} A_{11} & A_{12} & 0 & . \\ A_{21} & A_{22} & A_{23} & 0 \\ 0 & A_{32} & A_{33} & A_{34} \\ . & 0 & A_{43} & A_{44} \end{pmatrix} - A_{01}A_{10} \det \begin{pmatrix} A_{22} & A_{23} & 0 & . \\ A_{32} & A_{33} & A_{34} & 0 \\ 0 & A_{43} & A_{44} & A_{45} \\ . & 0 & A_{54} & A_{55} \end{pmatrix}\ . \tag{4.17}$$

Upon defining the determinant of the submatrix of A beginning with the i-th column and row, i.e.

$$D_i \stackrel{\text{def}}{=} \det \begin{pmatrix} A_{i,i} & A_{i,i+1} & 0 & . \\ A_{i+1,i} & A_{i+1,i+1} & A_{i+1,i+2} & 0 \\ 0 & A_{i+2,i+1} & A_{i+2,i+2} & A_{i+2,i+3} \\ . & 0 & A_{i+3,i+2} & A_{i+3,i+3} \end{pmatrix} \tag{4.18}$$

we can express the sought-for element of the inverse matrix (4.16) by

$$(A^{-1})_{00} = \frac{1}{\frac{D_0}{D_1}}\ .$$

We can now use (4.17) to express $\frac{D_0}{D_1}$

$$\frac{D_0}{D_1} = \frac{A_{00}D_1 - |A_{01}|^2 D_2}{D_1} = A_{00} - \frac{|A_{01}|^2}{D_1/D_2}$$

by $\frac{D_1}{D_2}$. Iterating the above reasoning yields

$$\frac{D_l}{D_{l+1}} = A_{ll} - \frac{|A_{ll+1}|^2}{D_{l+1}/D_{l+2}}\ ,$$

which leads to a continued fraction for the desired quantity

$$(A^{-1})_{00} = \frac{1}{D_0/D_1} = \cfrac{1}{A_{00} - \cfrac{|A_{01}|^2}{A_{11} - \cfrac{|A_{12}|^2}{A_{22} - \cfrac{|A_{23}|^2}{A_{33} - \ddots}}}} \; . \tag{4.19}$$

For we original problem $(w^+ \pm \hat{H})^{-1}_{00}$ the continued fraction reads

$$(w^+ \pm (\hat{H} - E_0))^{-1}_{00} = \cfrac{1}{w^+ \pm \Delta\varepsilon_0 - \cfrac{|k_1|^2}{w^+ \pm \Delta\varepsilon_1 - \cfrac{|k_2|^2}{w^+ \pm \Delta\varepsilon_2 \ddots}}} \tag{4.20}$$

This expression is well suited for numerical treatment and can be iterated for arbitrary w.

To this end, we introduce the abbreviations

$$\begin{aligned} d_i &= \omega^+ \pm \Delta\varepsilon_i \qquad && \text{for} \quad i = 0, 1, \ldots \\ e_i &= |k_i|^2 && \text{for} \quad i = 1, 2, \ldots \end{aligned}$$

Beginning with the upper left 2×2 submatrix of A the continued fraction has the form

$$\frac{1}{d_0 - \frac{e_1}{d_1 - R_1}} = \frac{d_1 - R_1}{d_0 d_1 - e_1 - d_0 R_1} =: \frac{a_1 + a_0 R_1}{b_1 + b_0 R_1} \; . \tag{4.21}$$

In the last equation we anticipated the general form. The remainder R_1 has again the form of a continued fraction. In general the remainder reads

$$R_i = \frac{e_{i+1}}{d_{i+1} - R_{i+1}} \; . \tag{4.22}$$

Upon substituting this for $i = 1$ into (4.21) we obtain

$$\frac{a_1 + a_0 R_1}{b_1 + b_0 R_1} = \frac{\overbrace{a_1 d_2 + a_0 e_2}^{a_1} + \overbrace{(-a_1)}^{a_0} R_2}{\underbrace{b_1 d_2 + b_0 e_2}_{b_1} + \underbrace{(-b_1)}_{b_0} R_2} \tag{4.23}$$

which is again of the form.

$$\frac{a_1 + a_0 R}{b_1 + b_0 R} \; . \tag{4.24}$$

Thus the iteration formula for $i = 1, 2, \ldots$ deduced from the above considerations is given by

$$\begin{aligned} a_1 &\longrightarrow a_1 d_{i+1} + a_0\, e_{i+1} \\ a_0 &\longrightarrow -a_1 \\ b_1 &\longrightarrow b_1 d_{i+1} + b_0\, e_{i+1} \\ b_0 &\longrightarrow -b_1 \ , \end{aligned}$$

with the initial values

$$a_1 = d_1, \quad a_0 = -1, \quad b_1 = d_0 d_1 - e_1, \quad b_0 = -d_0 \ . \tag{4.25}$$

The sequence is iterated for each ω individually and ends if the Krylov space is exhausted or if a desired convergency of

$$g(\omega) = \frac{a_1}{b_1}$$

is achieved. In order to avoid numerical instabilities, it is recommendable to rescale all quantities a_0, a_1, b_0, b_1 e.g. by $b_1 = 1$ after each iteration.

In some cases it may happen that the Green's function of interest is not diagonal in the operators, e.g.

$$g_{AB} = \left\langle \hat{A}^\dagger \frac{1}{w^+ - (\hat{H} - E_0)} \hat{B} \right\rangle \ .$$

In this case we define two operators $\hat{O}_\alpha = \hat{A} + \alpha \hat{B}$ and determine the diagonal Green's functions

$$g_\alpha = \left\langle \hat{O}_\alpha^\dagger \frac{1}{w^+ - (\hat{H} - E_0)} \hat{O}_\alpha \right\rangle \ .$$

It is easily possible to separate g_{AB} by linearly combining the four Green's functions for $\alpha = \{\pm 1, \pm i\}$.

4.2.5 Lehmann – Representation

Before considering some simple examples, we want to present an alternative way of calculating Green's functions, the so *Lehmann representaion*. Again we consider the matrix elements of the form

$$\langle \psi_0 | \, \hat{O}^\dagger \, \frac{1}{\omega^+ \pm (\hat{H} - E_0)} \, \hat{=} \, |\psi_0\rangle \, , \tag{4.26}$$

where $\hat{O}$ is some appropriate operator and $|\psi_0\rangle$ represents the ground state. Like before we define $|\varphi_0\rangle$ as the normalized vector $\hat{O}\,|\psi_0\rangle$, which serves as initial vector of a Lanczos sequence. We insert a complete orthonormal set of eigenvectors of $\hat{H}$ given by

$$\mathbb{I} = \sum_\nu |\psi_\nu\rangle\langle\psi_\nu| \ .$$

Then (4.26) can be cast into the form

$$\langle\psi_0|\, \hat{O}^\dagger \, \frac{1}{\omega^+ \pm (\hat{H} - E_0)} \, \hat{O}\, |\psi_0\rangle = \sum_\nu \frac{\langle\psi_0|\, \hat{O}^\dagger\, |\psi_\nu\rangle \, \langle\psi_\nu|\, \hat{O}\, |\psi_0\rangle}{\omega^+ \pm (E_\nu - E_0)} \ .$$

Next we expand the eigenvectors $|\psi_\nu\rangle$ in the Lanczos basis $\{|\varphi_i\rangle\}$

$$|\psi_\nu\rangle = \sum_i c_i^{(\nu)} \, |\varphi_i\rangle \, , \quad \text{with} \ \ c_i^{(\nu)} = \langle\varphi_i\, |\psi_\nu\,\rangle$$

to obtain

$$\begin{aligned}\langle\psi_\nu|\, \hat{O}\, |\psi_0\rangle &= \sum_i c_i^{(\nu)*} \langle\varphi_i| \underbrace{\hat{O}\, |\psi_0\rangle}_{\sim|\varphi_0\rangle} = \sqrt{\langle\psi_0|O^\dagger O|\psi_0\rangle} \sum_i c_i^{(\nu)*} \underbrace{\langle\varphi_i\, |\varphi_0\,\rangle}_{\delta_{i,0}} \\ &= \sqrt{\langle\psi_0|O^\dagger O|\psi_0\rangle}\, c_0^{(\nu)*} \ .\end{aligned}$$

This means that except of the first terms all summands vanish. Thus (4.26) can be approximated by

$$\langle\psi_0|\, \hat{O}^\dagger \, \frac{1}{\omega^+ \pm (\hat{H} - E_0)} \, \hat{O}\, |\psi_0\rangle \ = \ \langle\psi_0|O^\dagger O|\psi_0\rangle \sum_{\nu=1}^{N_L} \frac{|c_0^{(\nu)}|^2}{\omega^+ \pm (\tilde{E}_\nu - \tilde{E}_0)} \ , \tag{4.27}$$

where only the first components $c_0^{(\nu)}$ of the expansion of the eigenvector $|\psi_\nu\rangle$ in the Lanczos basis are required. In general, the eigenstates $|\psi_\nu\rangle$ ($\nu = 1, \ldots, N_L$), computed by the Lanczos procedure, do not form a complete set of basis vectors, nor are the respective energies $\tilde{E}_\nu$ exact eigenvalues of $\hat{H}$. However, with increasing number of iterations, the Lanczos procedure converges towards the exact Green's function and the convergency can be monitored and stopped as soon as the desired accuracy is reached. The approximate Lehmann representation (**??**) is an explicit sum of simple poles. The same holds true for the continued fraction, less obviously though.

4.2.6 Analytically treatable models

In this section we discuss a couple of simple examples in order to illustrate the Lanczos methods. We start out with various aspects of the tight binding Hamiltonian that accounts for nearest neighbor hopping of electrons. The model Hamiltonian for the one-dimensional lattice reads

$$\hat{H} = -t \sum_{\substack{<i,j> \\ \sigma}} a_{i\sigma}^\dagger \, a_{j\sigma} = \sum_{k,\sigma}^{1.\mathrm{bz}} \varepsilon_k \, a_{k\sigma}^\dagger a_{k\sigma} \ . \tag{4.28}$$

The operators $a_{i\sigma}^\dagger$ and $a_{i\sigma}$ create (annihilate) electrons in Wannier states centered at lattice site i. The dispersion relation follows from Fourier transformation

$$\varepsilon(k) = -2\,t\,\cos(k)\ . \tag{4.29}$$

The sum over k-vectors is restricted to the first Brillouin zone $k \in (-\pi, \pi]$.

One-Particle Green's function. For fermions it is expedient to choose the anticommutator Green's function, i.e. $\varepsilon = -1$.

$$\begin{aligned} g_{k\sigma}(w) &= \left\langle\left\langle a_{k\sigma}(t); a_{k\sigma}^\dagger(0)\right\rangle\right\rangle \\ &= \langle\psi_0|a_{k\sigma}\frac{1}{w^+ - (\hat{H}-E_0)}\,a_{k\sigma}^\dagger|\psi_0\rangle \\ &+ \langle\psi_0|a_{k\sigma}^\dagger\frac{1}{w^+ + (\hat{H}-E_0)}\,a_{k\sigma}|\psi_0\rangle\ , \end{aligned} \tag{4.30}$$

where the first term describes *inverse photo emission spectroscopy (IPES)* and the second one *photo emission spectroscopy (PES)*. As usual, $|\psi_0\rangle$ denotes the exact many-body system ground state.

Since we need normalized initial vectors for the Lanczos procedure, we write

$$\begin{aligned} a_{k\sigma}^\dagger\,|\psi_0\rangle &\stackrel{\text{def}}{=} \sqrt{\langle\psi|a_{k\sigma}a_{k\sigma}^\dagger|\psi_0\rangle}\,|\varphi_0\rangle = \sqrt{1-n_{k\sigma}}\,|\varphi_0\rangle \\ a_{k\sigma}\,|\psi_0\rangle &\stackrel{\text{def}}{=} \sqrt{\langle\psi|a_{k\sigma}^\dagger a_{k\sigma}|\psi_0\rangle}\,|\tilde{\varphi}_0\rangle = \sqrt{n_{k\sigma}}\,|\tilde{\varphi}_0\rangle \end{aligned} \tag{4.31}$$

and obtain factors involving the particle numbers $n_{k\sigma}$. The Green's function suitable for the Lanczos treatment reads

$$\begin{aligned} g_{k\sigma}(\omega) =& (1-n_{k\sigma})\left\langle\varphi_0\right|\frac{1}{\omega^+ - (\hat{H}-E_0)}\left|\varphi_0\right\rangle \\ &+ n_{k\sigma}\left\langle\tilde{\varphi}_0\right|\frac{1}{\omega^+ + (\hat{H}-E_0)}\left|\tilde{\varphi}_0\right\rangle\ . \end{aligned} \tag{4.32}$$

The Green's function has the asymptotic behavior

$$\lim_{\omega\to\infty} g_{k\sigma}(\omega) = \frac{1-n_{k\sigma}}{\omega^+} + \frac{n_{k\sigma}}{\omega^+} = \frac{1}{\omega^+}\ . \tag{4.33}$$

We start out with the Lanczos iteration for the *IPES* Green's function

$$\begin{aligned} H\,|\varphi_0\rangle &= (1-n_{k\sigma})^{-1/2}\hat{H}\,a_{k\sigma}^\dagger|\psi_0\rangle \\ &= (1-n_{k\sigma})^{-1/2}\left(a_{k\sigma}^\dagger\hat{H} + \left[\hat{H}, a_{k\sigma}^\dagger\right]\right)|\psi_0\rangle \\ &= (1-n_{k\sigma})^{-1/2}\Big(a_{k\sigma}^\dagger\,\underbrace{\hat{H}|\psi_0\rangle}_{E_0|\psi_0\rangle} + \varepsilon_k\,a_{k\sigma}^\dagger\,|\psi_0\rangle\Big) \\ &= (E_0+\varepsilon_k)\,|\varphi_0\rangle \end{aligned}$$

For the last equation we have used the first of the identities

$$\left[\hat{H}, a^\dagger_{k\sigma}\right] = \varepsilon_k\, a^\dagger_{k\sigma} \;, \qquad \left[\hat{H}, a_{k\sigma}\right] = -\varepsilon_k\, a_{k\sigma} \tag{4.34}$$

that follow directly from the specific form of the Hamiltonian and the fermionic anticommutator relations. Since the tight binding Hamiltonian describes interaction-free electrons, $|\varphi_0\rangle$ is already an eigenstate of $\hat{H}$ and we have

$$\begin{aligned} \varepsilon_0 = \langle\varphi_0|\hat{H}|\varphi_0\rangle \quad &= E_0 + e_k \\ \left|\tilde{\varphi}_1\right\rangle = \hat{H}\,|\varphi_0\rangle - \varepsilon_0|\varphi_0\rangle \quad &= 0 \;, \end{aligned}$$

and the Lanczos procedure ends immediately. The *IPES* part of (4.32) is given by a single pole

$$g^+_{k\sigma}(\omega) \stackrel{\text{def}}{=} (1 - n_{k\sigma}) \left\langle \varphi_0 \left| \frac{1}{\omega^+ - (\hat{H} - E_0)} \right| \varphi_0 \right\rangle = \frac{1 - n_{k\sigma}}{\omega^+ - \varepsilon_k} \;. \tag{4.35}$$

In the same manner one can deduce the *PES* term of (4.32)

$$g^-_{k\sigma}(\omega) \stackrel{\text{def}}{=} n_{k\sigma} \left\langle \tilde{\varphi}_0 \left| \frac{1}{\omega^+ + (\hat{H} - E_0)} \right| \tilde{\varphi}_0 \right\rangle = \frac{n_{k\sigma}}{\omega^+ - \varepsilon_k} \;. \tag{4.36}$$

Adding both contributions, the one-particle Green's function is finally given by

$$g_{k\sigma}(\omega) = \frac{1}{\omega^+ - \varepsilon_k} \;.$$

Density of states of the tight-binding model. In this section we will compute the of states (DOS) $\rho(\omega)$ of the tight binding model in 1-d. Before employing the Lanczos procedure, we will determine $\rho(\omega)$ analytically. This example, though embarrassingly trivial in k-space, is very interesting in real space, since it illustrates how a finite imaginary part comes about in the thermodynamic limit, even though any finite number of Lanczos iterations yields a superposition of δ-function peaks.

The Hamiltonian of the 1d-tight-binding model is given by (4.28). Expressing energies in units of $|t|$ the dispersion relation is

$$\varepsilon(k) = -2\,\cos(k) \;. \tag{4.37}$$

The density of states (DOS) of non-interacting electrons can be computed via

$$\rho(\omega) \stackrel{\text{def}}{=} \frac{1}{N} \sum_{n=1}^{N} \delta(\omega - \varepsilon(k_n))$$

where k_n, given by

$$k_n = \frac{2\pi}{N} n \quad n = 1, \ldots, N \ ,$$

covers the first Brillouin zone. In the thermodynamic limit ($N \to \infty$) the sum approaches

$$\rho(\omega) \underset{N\to\infty}{\longrightarrow} \frac{1}{\pi} \int_0^{\pi} \delta(\omega - \varepsilon(k))\, dk \ ,$$

where inversion symmetry of the dispersion relation has been exploited. Since $\omega - \varepsilon(k)$ has only simple roots k^* in the interval $[0, \pi)$, we obtain

$$\int_0^{\pi} \delta(\omega + 2\cos(k))\, dx = \frac{1}{|\frac{\mathrm{d}}{\mathrm{d}k} 2\cos(k)|_{k^*}} = \frac{1}{2|\sin(k^*)|} \ .$$

The 1-d tight binding DOS is therefore

$$\rho(\omega) = \frac{1}{2\pi} \begin{cases} \frac{1}{\sqrt{1-(w/2)^2}} & \text{if } \left|\frac{\omega}{2}\right| \le 1 \\ 0 & \text{otherwise} \end{cases} \ .$$

The density of states is depicted in Fig. 4.2.6. It exhibits well known van-Hove

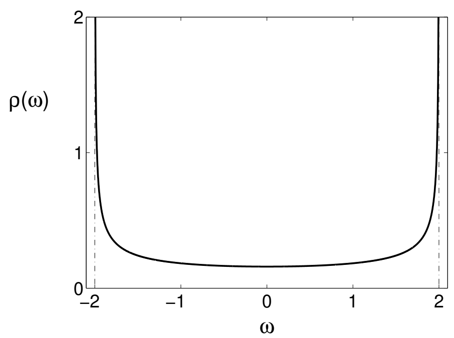

Fig. 4.3. Density of states (DOS) of the one-dimensional tight-binding model

singularities for energies near the band edges $\omega = \pm 2$.

Now we will use the real space representation to directly determine $\rho(\omega)$ via the Lanczos algorithm. The density of states is related to the one-particle Green's function by

$$\rho(\omega) = -\frac{1}{\pi} \Im \frac{1}{N} \sum_k g^{\sigma}_{kk}(\omega) = -\frac{1}{\pi} \Im \frac{1}{N} \sum_i g^{\sigma}_{ii}(\omega) = -\frac{1}{\pi} \Im \left\langle\!\left\langle a_{i\sigma}; a^{\dagger}_{i\sigma} \right\rangle\!\right\rangle_w ,$$

where the invariance of the trace against unitary transformations and the translational invariance of the Hamiltonian has been used.

We now apply the Lanczos method to calculate g^{σ}_{ii}. We will see that the result is indeed independent of the site index i. In the present, interaction-free, case the result does not dependent upon the particle number of the reference many-body ground state $|\psi_0\rangle$. We can simplify the computation by choosing the vacuum state as reference state, i.e. $|\psi_0\rangle = |0\rangle$. Therefore, we avoid the ground state computation and proceed with the Lanczos procedure for the dynamical correlation function. The initial vector reads

$$|\varphi_0\rangle = \hat{a}^{\dagger}_{i\sigma}\,|0\rangle \overset{\text{def}}{=} |i\rangle\ .$$

where the particle has been transferred to the neighboring sites. This state is already orthogonal to $|\varphi_0\rangle$. Normalization yields

$$|\varphi_1\rangle = \frac{1}{\sqrt{2}}\left(|i+1\rangle + \,|i-1\rangle\right)\ .$$

The second Lanczos iteration leads to

$$\begin{aligned}\left|\tilde{\varphi}_2\right\rangle = \hat{H}\,|\varphi_1\rangle &= -\frac{t}{\sqrt{2}}\left(\hat{H}\,|i+1\rangle + \hat{H}\,|i-1\rangle\right)\\ &= -\frac{t}{\sqrt{2}}\left(|i+2\rangle + \,|i\rangle + \,|i\rangle + \,|i-2\rangle\right)\ .\end{aligned}$$

Upon discarding the components of this state parallel to the $|\varphi_0\rangle$ and $|\varphi_1\rangle$ we obtain after normalization

$$|\varphi_1\rangle = \frac{1}{\sqrt{2}}\left(|i+2\rangle + \,|i-2\rangle\right)\ .$$

It appears that the general form of $|\varphi_l\rangle$ is given by the hopping over l lattice sites

$$|\varphi_l\rangle = \frac{1}{\sqrt{2}}\left(|i+l\rangle + \,|i-l\rangle\right)\ .$$

Calculation of ε_i and k_i is straight forward and yields

$$\begin{aligned}\varepsilon_i &= 0\\ k_i &= \begin{cases}\sqrt{2} & \text{for } i=1\\ 1 & \text{otherwise}\end{cases}\end{aligned} \tag{4.38}$$

Therefore the continued fraction has the structure

$$g_{ii}(\omega) = \cfrac{1}{\omega - 2\cfrac{1}{\omega - \cfrac{1}{\omega - \cfrac{1}{\omega - \cdots}}}}\ .$$

The structure is sufficiently simple to allow an a explicit summation of the continued fraction. We define the quantity

$$G(\omega) = \cfrac{1}{\omega - \cfrac{1}{\omega - \cfrac{1}{\omega - \cdots}}} \tag{4.39}$$

which is self similar and fulfils the equation

$$G(\omega) = \frac{1}{\omega - G(\omega)} \, .$$

The solution for G is given by

$$G(\omega) = \frac{\omega}{2} \pm \sqrt{\frac{\omega^2}{4} - 1} \, .$$

There are two solutions to this equation, although the original continued fraction (4.39) has a unique value. According to (4.33) one solution can be ruled out and the sought-for Green's functions reads

$$g_{ii}(\omega) = \frac{1}{\omega - 2\,G(\omega)} = \frac{1}{\sqrt{\omega^2 - 4}} \, .$$

Thus the spectral density is

$$\rho_{ii}(\omega) = -\frac{1}{\pi}\,\Im\, g_{ii}(\omega) = -\frac{1}{\pi}\,\Im\,\frac{1}{\sqrt{\omega^2 + 2i\delta\omega - 4}} = \begin{cases} \frac{1}{\pi}\,\frac{1}{\sqrt{4-\omega^2}} & \text{for } \omega^2 < 4 \\ 0 & \text{otherwise} \end{cases}$$

In the final step $\delta \to 0$ has been performed. As mentioned in the beginning, the continuous imaginary part of g_{ii} occurs only in the thermodynamic limit of infinite systems. If the procedure is terminated after n Lanczos iterations, the Green's function constitutes a sum of n simple poles. The results of the first iterations are

$$\begin{aligned} g_{ii}^{(1)}(\omega^+) &= \frac{1}{\omega^+} \\ g_{ii}^{(2)}(\omega^+) &= \cfrac{1}{\omega^+ - \cfrac{2}{\omega^+}} = \frac{1}{2}\left(\frac{1}{\omega^+ - \sqrt{2}} + \frac{1}{\omega^+ + \sqrt{2}}\right) \end{aligned}$$

$$
\begin{aligned}
g_{ii}^{(3)}(\omega^+) =& \cfrac{1}{\omega^+ - \cfrac{2}{\omega^+ - \cfrac{1}{\omega^+}}} = \frac{{\omega^+}^2 - 1}{\omega^+({\omega^+}^2 - 3)} \\
=& \frac{1}{3}\left(\frac{1}{\omega^+} + \frac{1}{\omega^+ + \sqrt{3}} + \frac{1}{\omega^+ - \sqrt{3}}\right) \\
&\vdots \\
g_{ii}^{(n)}(\omega^+) =& \sum_{\nu=1}^{n} \frac{c_\nu}{\omega^+ - \omega_\nu} \qquad\qquad c_\nu, \omega_\nu \in \mathbb{R}
\end{aligned}
\tag{4.40}
$$

The plots in Fig. 4.4 show the results for ρ obtained by different numbers n

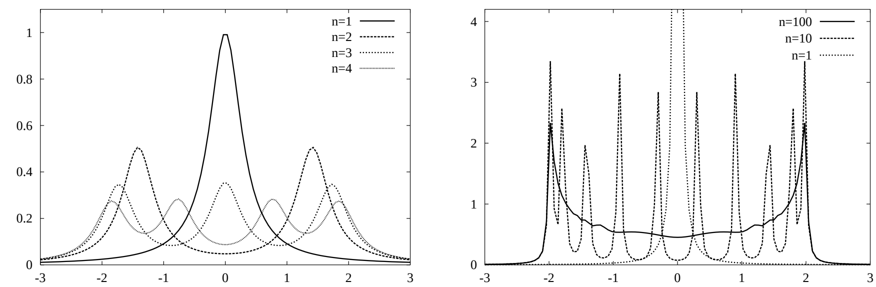

Fig. 4.4. Densities $\rho(\varepsilon)$ obtained by different numbers of Lanczos iterations. The value for the lifetime broadening is $\delta = 0.1$ in the left panel and $\delta = 0.03$ in the right panel.

of Lanczos steps. For any finite n the imaginary part of the Green's function is a superposition of delta functions, corresponding to infinite lifetime of the quasi particles. For a finite number n of Lanczos steps, which in the present example is equivalent to a finite system of size n, we have to choose a reasonable finite value for δ which represents a tradeoff between artificial finite size structure and loss of resolution. The results in Fig. 4.4 approach systematically the exact thermodynamic result of Fig 4.2.6.

This example illustrates, that the Krylov space, generated by the Hamiltonian, is optimal as far as total energy is concerned. Convergence of general correlation functions can be considerably slower. After l iterations the lowest Lanczos eigenvector is approximately

$$
\left|\Psi_0^L\right\rangle \propto \sum_{j=-l}^{l} a_{l+i}^\dagger |0\rangle \ ,
$$

which is nearly correct for the sites $(i-l, \ldots, i+l$ reached during the Lanczos iteration. Contributions from outside this regime are zero. This is, however, not really a problem for many-particle models, since in these aplicatiosns tractable system sizes are fairly small anyways.

4.2.7 The Hubbard Model for two sites

Next we consider the Hubbard model for two sites $x_1 = 0$ and $x_2 = 1$ with the Hamiltonian

$$H = \underbrace{-t\left\{a^\dagger_{1\uparrow}a_{2\uparrow} + a^\dagger_{2\uparrow}a_{1\uparrow} + a^\dagger_{1\downarrow}a_{2\downarrow} + a^\dagger_{2\downarrow}a_{1\downarrow}\right\}}_{\hat{H}_{\text{kin}}} + \underbrace{U\left(\hat{n}_{1\uparrow}\hat{n}_{1\downarrow} + \hat{n}_{2\uparrow}\hat{n}_{2\downarrow}\right)}_{\hat{H}_{\text{int}}} .$$

The goal of this section is the evaluation of the one-particle Green's function $\langle\langle a_{k\uparrow}; a^\dagger_{k\uparrow}\rangle\rangle$ at half-filling, since here the correlation effects are most significant. The Green's function reads

$$\begin{aligned} g_k(\omega) := \langle\langle a_{k\uparrow}; a^\dagger_{k\uparrow}\rangle\rangle_\omega =& \langle\psi_0|\, a_{k\uparrow}\, \frac{1}{\omega^+ - (\hat{H} - E_0)} a^\dagger_{k\uparrow}|\psi_0\rangle \\ & - \langle\psi_0|\, a^\dagger_{k\uparrow}\, \frac{1}{\omega^+ + (\hat{H} - E_0)} a_{k\uparrow}|\psi_0\rangle \ , \end{aligned} \tag{4.41}$$

with the ground-state vector $|\psi_0\rangle$ of the half-filled system. For two sites half-filling means one $\uparrow$- and one $\downarrow$-electron. For the Lanczos procedure we first need the exact many-body ground state $|\psi_0\rangle$ for half-filling. The initial vector $a^\dagger_{k\uparrow}|\psi_0\rangle$ for the IPES process involves states with two $\uparrow$- and one $\downarrow$-electrons, whereas the initial state $a_{k\uparrow}|\psi_0\rangle$ for the PES process involves states with one $\downarrow$-electron.

We first calculate explicitly the eigenvalues and eigenvectors of the Hamiltonian for the above-mentioned occupation numbers

One spin $\downarrow$ electron. The two basis vectors are

$$\begin{aligned} |\varphi_1\rangle &= a^\dagger_{1\downarrow}\,|0\rangle \\ |\varphi_2\rangle &= a^\dagger_{2\downarrow}\,|0\rangle\,. \end{aligned}$$

The action of the Hamiltonian on these state vectors is

$$\begin{aligned} \hat{H}_{\text{kin}}\,|\varphi_1\rangle &= -t\,a^\dagger_{2\downarrow}|0\rangle = -t\,|\varphi_2\rangle \\ \hat{H}_{\text{kin}}\,|\varphi_2\rangle &= -t\,a^\dagger_{1\downarrow}|0\rangle = -t\,|\varphi_1\rangle \\ \hat{H}_{\text{int}}\,|\varphi_1\rangle &= 0 \\ \hat{H}_{\text{int}}\,|\varphi_2\rangle &= 0\ . \end{aligned}$$

Since there is only one electron, there is no partner to interact with and the interaction energy is zero. In the basis $\{|\varphi_1\rangle, |\varphi_2\rangle\}$ the Hamiltonian reads

$$H = \begin{pmatrix} 0 & -t \\ -t & 0 \end{pmatrix} \tag{4.42}$$

and has the following eigenvalues and normalized eigenvectors:

$$E_1^{(1)} = -t \ : \qquad \left|\Psi_1^{(1)}\right\rangle = \frac{1}{\sqrt{2}}\left(|\varphi_1\rangle + |\varphi_2\rangle\right) \tag{4.43}$$

$$E_2^{(1)} = +t \ ; \qquad \left|\Psi_2^{(1)}\right\rangle = \frac{1}{\sqrt{2}}\left(|\varphi_1\rangle - |\varphi_2\rangle\right) \ . \tag{4.44}$$

The eigenvectors are Bloch states

$$\left|\Psi_j^{(1)}\right\rangle = \frac{1}{\sqrt{2}}\sum_{i=1}^{2} \mathrm{e}^{\mathrm{i}k_j x_i}\,|\varphi_i\rangle \ ,$$

corresponding to $k = 0$ and $k = \pi$.

Two spin ↑ electrons (half-filling). The case of two spin up – or equivalently two spin down – electrons is not very interesting in itself. Due to the Pauli exclusion principle, hopping is prohibited. The only allowed state vector reads

$$|\xi\rangle = a_{1\uparrow}^{\dagger} a_{2\uparrow}^{\dagger} |0\rangle \ .$$

This vector is already an eigenstate of the Hamiltonian with eigenvalue zero

$$\hat{H}\,|\xi\rangle = \hat{H}_{\mathrm{kin}}\,|\xi\rangle + \hat{H}_{\mathrm{int}}\,|\xi\rangle = (0\,+\,0)\,|\xi\rangle \ .$$

Thus two spin-↑ electrons have energy $E^{(\uparrow\uparrow)} = 0$.

The reason of our treating this case lies in the comparison with the spin-↑↓ state. As we will see in the following paragraph, in the latter case the possibility of virtual hopping processes reduces the ground-state energy of the system. Thus, for half-filling, the Hubbard model favors antiferromagnetism, at least as far as short range correlations are concerned

One spin ↑ and one spin ↓ electron (half-filling). In the half-filled case there are four basis states

$$|\chi_1\rangle = a_{1\uparrow}^{\dagger} a_{2\downarrow}^{\dagger} |0\rangle \ ; \qquad |\chi_2\rangle = a_{2\uparrow}^{\dagger} a_{1\downarrow}^{\dagger} |0\rangle$$

$$|\chi_3\rangle = a_{1\uparrow}^{\dagger} a_{1\downarrow}^{\dagger} |0\rangle \ ; \qquad |\chi_4\rangle = a_{2\uparrow}^{\dagger} a_{2\downarrow}^{\dagger} |0\rangle \ .$$

Application of the Hamiltonian yields

$$\hat{H}_{\mathrm{kin}}\,|\chi_1\rangle = -t\{|\chi_3\rangle + |\chi_4\rangle\} \ ; \qquad \hat{H}_{\mathrm{int}}\,|\chi_1\rangle = 0$$

$$\hat{H}_{\mathrm{kin}}\,|\chi_2\rangle = -t\{|\chi_3\rangle + |\chi_4\rangle\} \ ; \qquad \hat{H}_{\mathrm{int}}\,|\chi_2\rangle = 0$$

$$\hat{H}_{\mathrm{kin}}\,|\chi_3\rangle = -t\{|\chi_1\rangle + |\chi_2\rangle\} \ ; \qquad \hat{H}_{\mathrm{int}}\,|\chi_3\rangle = U\,|\chi_3\rangle$$

$$\hat{H}_{\mathrm{kin}}\,|\chi_4\rangle = -t\{|\chi_1\rangle + |\chi_2\rangle\} \ ; \qquad \hat{H}_{\mathrm{int}}\,|\chi_4\rangle = U\,|\chi_4\rangle \ .$$

Therefore, the Hamiltonian matrix reads

$$H = \begin{pmatrix} 0 & 0 & -t & -t \\ 0 & 0 & -t & -t \\ -t & -t & U & 0 \\ -t & -t & 0 & U \end{pmatrix} . \tag{4.45}$$

It has the structure

$$H = \begin{pmatrix} \mathcal{O} & \mathcal{T} \\ \mathcal{T} & \mathcal{U} \end{pmatrix} \quad \text{with } \mathcal{T} = -\begin{pmatrix} t & t \\ t & t \end{pmatrix} , \ \mathcal{O} = \begin{pmatrix} 0 & 0 \\ 0 & 0 \end{pmatrix} , \ \mathcal{U} = \begin{pmatrix} U & 0 \\ 0 & U \end{pmatrix} .$$

By denoting the eigenvector as (x_1, x_2, y_1, y_2), we can split the eigenvalue problem into two parts:

$$\mathcal{T}\boldsymbol{y} = E\boldsymbol{x} \tag{4.46a}$$

$$\mathcal{T}\boldsymbol{x} + U\boldsymbol{y} = E\boldsymbol{y} \tag{4.46b}$$

Provided $E \neq 0$ we can eliminate $\boldsymbol{x}$ by substituting (4.46a) into (4.46b)

$$\left(\mathcal{T}^2 - E^2 + EU\right)\boldsymbol{y} = \left(2\,t^2 \begin{pmatrix} 1 & 1 \\ 1 & 1 \end{pmatrix} - E^2 + EU\right)\boldsymbol{y} = 0 . \tag{4.47}$$

The eigenvectors are given by

$$\boldsymbol{y}_1 = \frac{1}{\sqrt{2}} \begin{pmatrix} 1 \\ 1 \end{pmatrix} \qquad \text{and} \qquad \boldsymbol{y}_2 = \frac{1}{\sqrt{2}} \begin{pmatrix} 1 \\ -1 \end{pmatrix} \tag{4.48}$$

and the corresponding equations (4.47) for the eigenvalues are

$$\begin{aligned}
\boldsymbol{y}_1 : \quad & \left(4t^2 - E^2 + EU\right) = 0 \quad \Rightarrow \quad & E_1 &= \tfrac{U}{2} - \sqrt{\left(\tfrac{U}{2}\right)^2 + 4t^2} \\
& & E_4 &= \tfrac{U}{2} + \sqrt{\left(\tfrac{U}{2}\right)^2 + 4t^2} \\
\boldsymbol{y}_2 : \quad & \left(-E^2 + EU\right) = 0 \quad \Rightarrow \quad & E_2 &= 0 \\
& & E_3 &= U .
\end{aligned}$$

The ground-state energy

$$E_0^{(2)} = \tfrac{U}{2} - \sqrt{\left(\tfrac{U}{2}\right)^2 + 4t^2} \tag{4.49}$$

corresponds to $\boldsymbol{y} = \frac{1}{\sqrt{2}}(1\,,\,1)^T$. Along with (4.46a) we obtain $\boldsymbol{x} = -\frac{2t}{E_1}\,\boldsymbol{y}$ and the entire eigenvector $\boldsymbol{c}$ of the Hamilton matrix (4.45) reads

$$\begin{aligned}
\boldsymbol{c} &= \frac{1}{\sqrt{2(1+\kappa^2)}}\,\left(1, 1, \kappa, \kappa\right)^T \\
\kappa &= -\frac{E_1}{2t}
\end{aligned}$$

which corresponds to the ground-state vector

$$\left|\Psi_0^{(2)}\right\rangle = \frac{1}{\sqrt{2(1+\kappa^2)}}\left(a^\dagger_{1\uparrow}a^\dagger_{2\downarrow} + a^\dagger_{2\uparrow}a^\dagger_{1\downarrow} + \kappa\, a^\dagger_{1\uparrow}a^\dagger_{1\downarrow} + \kappa\, a^\dagger_{2\uparrow}a^\dagger_{2\downarrow}\right)|0\rangle\ , \quad (4.50)$$

which is a vector with total wavevector $k = 0$. For completeness we want to point out that the solution $E_2 = 0$ has to be treated separately. The only choice to fulfill (4.46a) is $\boldsymbol{y} = 0$. (4.46b) yields $\boldsymbol{x} = (1, -1)^T$.

4.2.8 Remark: Discussion of half-filling

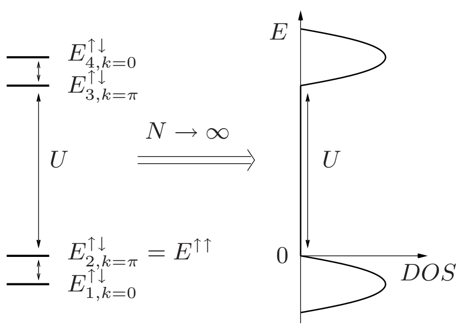

Fig. 4.5. Energy spectrum of the two-site Hubbard model (left) and density of states in the thermodynamic limit (right).

As already mentioned above, the ground-state energy of antiparallel spins is lower than that of parallel spins. Thus antiferromagnetic order is favored. The two lowest energies are composed predominantly of singly occupied basis states, while the two high energy states are characterized by pronounced double occupancies. The two energy regimes form the lower and upper Hubbard bands in the thermodynamic limit. The total wavevector of the states is included in Fig. 4.5.

In the physically interesting case of strong on-site repulsion ($U \gg |t|$), the square root can be expanded to first order

$$E^{(\uparrow\downarrow)}_{1,k=0} = -\frac{4t^2}{U} \quad , \qquad E^{(\uparrow\downarrow)}_{3,k=\pi} = U\ ,$$
$$E^{(\uparrow\downarrow)}_{2,k=\pi} = 0 \quad , \qquad E^{(\uparrow\downarrow)}_{4,k=0} = U + \frac{4t^2}{U}\ .$$

As illustrated in Fig. 4.5, we can distinguish two types of excitations, which preserve the particle number: The first ones are spin–wave excitations whose energy scale is set by the exchange coupling $J \propto t^2/U$. The second type are charge excitations with the energy scale U that involve doubly occupied sites.

In the absence of correlations ($U = 0$) which corresponds to the opposite limit, we obtain for the energies of the spin-$\uparrow\downarrow$ system

$$\begin{aligned} E_1^{(\uparrow\downarrow)} &= -2t \quad , \qquad & E_3^{(\uparrow\downarrow)} &= 0 \; , \\ E_2^{(\uparrow\downarrow)} &= 0 \quad , \qquad & E_4^{(\uparrow\downarrow)} &= 2t \; . \end{aligned}$$

In the thermodynamic limit, these energies form the tight binding band ((4.37)), which is is half filled and therefore represents a ideal metal. The strong local Coulomb repulsion drives a Metal insulator transition.

Two spin $\uparrow$ electrons and one spin $\downarrow$ electron. In order to determine the one-particle Green's function we still need the results for two spin $\uparrow$ electrons and one spin $\downarrow$ electron. The basis states for this case are

$$\begin{aligned} |\zeta_1\rangle &= a^\dagger_{1\uparrow} a^\dagger_{1\downarrow} a^\dagger_{2\uparrow} |0\rangle \\ |\zeta_2\rangle &= a^\dagger_{1\uparrow} a^\dagger_{2\uparrow} a^\dagger_{2\downarrow} |0\rangle \; . \end{aligned}$$

The Hamiltonian acts on the basis states as

$$\begin{aligned} \hat{H}_{\mathrm{kin}} \, |\zeta_1\rangle &= +t \; a^\dagger_{1\uparrow} a^\dagger_{2\uparrow} a^\dagger_{2\downarrow} \, |0\rangle \; = t \, |\zeta_2\rangle \\ \hat{H}_{\mathrm{kin}} \, |\zeta_2\rangle &= +t \; a^\dagger_{1\uparrow} a^\dagger_{2\uparrow} a^\dagger_{1\downarrow} \, |0\rangle \; = t \, |\zeta_1\rangle \\ \hat{H}_{\mathrm{int}} \, |\zeta_1\rangle &= U \, |\zeta_1\rangle \\ \hat{H}_{\mathrm{int}} \, |\zeta_2\rangle &= U \, |\zeta_2\rangle \; . \end{aligned}$$

Thus the Hamiltonian matrix in this basis is given by

$$H = \begin{pmatrix} U & t \\ t & U \end{pmatrix} \; . \tag{4.51}$$

The corresponding eigenvalues and eigenvectors are

$$E_1^{(3)} = U - t \; , \qquad \left|\Psi_1^{(3)}\right\rangle = \frac{1}{\sqrt{2}} \left(|\zeta_1\rangle - |\zeta_2\rangle\right) \; , \tag{4.52}$$

$$E_2^{(3)} = U + t \; , \qquad \left|\Psi_2^{(3)}\right\rangle = \frac{1}{\sqrt{2}} \left(|\zeta_1\rangle + |\zeta_2\rangle\right) \; . \tag{4.53}$$

The two states correspond again to total wavevector $k = \pi$ and $k = 0$, respectively. The result could have been derived more elegantly by particle-hole symmetry.

One-Particle Green's Function. Now we have all necessary information to evaluate the one-particle Green's function $g_{k\sigma}(\omega)$ via the Lanczos procedure. The Fourier transformed fermion operators are in the two-site case simply

$$a^\dagger_{k\uparrow} = \frac{1}{\sqrt{2}} \left(a^\dagger_{1\uparrow} \pm a^\dagger_{2\uparrow}\right) \qquad a_{k\uparrow} = \frac{1}{\sqrt{2}} \left(a_{1\uparrow} \pm a_{2\uparrow}\right) \; . \tag{4.54}$$

The upper sign stands for $k = 0$ and the lower sign for $k = \pi$. For the Green's function given in (4.41) we need the vector

$$\begin{aligned}
|\chi_0\rangle &\stackrel{\text{def}}{=} a^\dagger_{k\uparrow}|\psi_0\rangle = \frac{1}{\sqrt{2}}\left(a^\dagger_{1\uparrow} \pm a^\dagger_{2\uparrow}\right)|\psi_0\rangle \\
&= \frac{1}{\sqrt{2}Z}\left(a^\dagger_{1\uparrow} \pm a^\dagger_{2\uparrow}\right)\left(a^\dagger_{1\uparrow}a^\dagger_{2\downarrow} + a^\dagger_{2\uparrow}a^\dagger_{1\downarrow} + \kappa\, a^\dagger_{1\uparrow}a^\dagger_{1\downarrow} + \kappa\, a^\dagger_{2\uparrow}a^\dagger_{2\downarrow}\right)|0\rangle \\
&= \frac{1}{\sqrt{2}Z}\left(a^\dagger_{1\uparrow}a^\dagger_{2\uparrow}a^\dagger_{1\downarrow} + \kappa\, a^\dagger_{1\uparrow}a^\dagger_{2\uparrow}a^\dagger_{2\downarrow} \pm a^\dagger_{2\uparrow}a^\dagger_{1\uparrow}a^\dagger_{2\downarrow} \pm \kappa\, a^\dagger_{2\uparrow}a^\dagger_{1\uparrow}a^\dagger_{1\downarrow}\right)|0\rangle \\
&= \frac{1 \mp \kappa}{\sqrt{2}Z}\left(a^\dagger_{1\uparrow}a^\dagger_{2\uparrow}a^\dagger_{1\downarrow} \mp a^\dagger_{1\uparrow}a^\dagger_{2\uparrow}a^\dagger_{2\downarrow}\right)|0\rangle \\
&= \frac{1 \mp \kappa}{\sqrt{2}Z}\left(|\zeta_1\rangle \mp |\zeta_2\rangle\right) = \frac{1 \mp \kappa}{Z}\,|\Psi^{(3)}_{1/2}\rangle
\end{aligned}$$

where we have introduced the abbreviation $Z = \sqrt{2(1+\kappa^2)}$. For the PES process we need

$$\begin{aligned}
|\chi'_0\rangle &\stackrel{\text{def}}{=} a_{k\uparrow}|\psi_0\rangle = \frac{1}{\sqrt{2}}\left(a_{1\uparrow} \pm a_{2\uparrow}\right)|\psi_0\rangle \\
&= \frac{1}{\sqrt{2}Z}\left(a_{1\uparrow} \pm a_{2\uparrow}\right)\left(a^\dagger_{1\uparrow}a^\dagger_{2\downarrow} + a^\dagger_{2\uparrow}a^\dagger_{1\downarrow} + \kappa\, a^\dagger_{1\uparrow}a^\dagger_{1\downarrow} + \kappa\, a^\dagger_{2\uparrow}a^\dagger_{2\downarrow}\right)|0\rangle \\
&= \frac{1}{\sqrt{2}Z}\left(a^\dagger_{2\downarrow} + \kappa\, a^\dagger_{1\downarrow} \pm a^\dagger_{1\downarrow} \pm \kappa\, a^\dagger_{2\downarrow}\right)|0\rangle \\
&= \frac{\kappa \pm 1}{\sqrt{2}Z}\left(|\varphi_1\rangle \pm |\varphi_2\rangle\right) = \frac{\kappa \pm 1}{\sqrt{Z}}\,|\Psi^{(1)}_{2/1}\rangle\,.
\end{aligned}$$

Both, $|\chi_0\rangle$ and $|\chi'_0\rangle$ are therefore eigenvectors of the Hamiltonian for the three-particle and one-particle system, respectively, and the Lanczos procedure terminates after the first iteration. We obtain

$$\left\langle \chi_0 \middle| \frac{1}{\omega^+ - (\hat{H} - E_0)} \middle| \chi_0 \right\rangle = \frac{(1+\kappa)^2}{Z^2}\,\frac{1}{\omega^+ - (E^{(3)}_{2/1} - E^{(2)}_0)}\,.$$

The energy denominator of the IPES part yields

$$\omega^+ - (E^{(3)}_{2/1} - E^{(2)}_0) = \omega^+ - \left(\frac{U}{2} \pm t - \sqrt{(\tfrac{U}{2})^2 + 4t^2}\right)$$

Equivalently, we obtain for the PES part

$$\left\langle \chi'_0 \middle| \frac{1}{\omega^+ + (\hat{H} - E_0)} \middle| \chi'_0 \right\rangle = \frac{(1-\kappa)^2}{2(1+\kappa^2)}\,\frac{1}{\omega^+ + \left(E^{(1)}_{1/2} - E^{(2)}_0\right)}\,,$$

with an energy denominator

$$\begin{aligned}\omega^+ + \left(E^{(1)}_{1/2} - E^{(2)}_0\right) &= \omega^+ + \left(\mp t - \frac{U}{2} - \sqrt{(\tfrac{U}{2})^2 + 4t^2}\right) \\ &= \omega^+ - \left(\frac{U}{2} \pm t + \sqrt{(\tfrac{U}{2})^2 + 4t^2}\right) .\end{aligned}$$

In the strong coupling limit the excitation energies (poles) are ($U \gg |t|$)

$$\begin{aligned}\omega^+ &= \frac{U}{2} \pm t + \sqrt{\frac{U^2}{4} + 4\,t^2} \approx U \pm t + \frac{4\,t^2}{U} \\ \omega^+ &= \frac{U}{2} \pm t - \sqrt{\frac{U^2}{4} + 4\,t^2} \approx \pm t - \frac{4\,t^2}{U} .\end{aligned}$$

The IPES part describes the transition from the half-filled ground state to state with an additional electron. The excitation energy is dominated by U and describes inter-band transition. In photoemission an electron is removed from the half-filled ground state. The energy is of order t and corresponds to intra-band transition and decreases like $1/N$, while the inter-band energy remains of the order U.

One-Particle Green's function on the Bethe lattice. Eventually, we consider a less trivial example, namely non-interacting electrons on a Bethe lattice (Cayley tree), as depicted in Fig.4.6. A diagrammatic approach is given by Economou [**?**]. The Bethe lattice is characterized by the number Z of nearest neighbors and the fact that a particle can only return to a given site if it retraces the path on which it left the particular site. Or equivalently, if we cut a bond, the lattice disintegrates into two disconnected parts. A special case is $Z = 2$ which is identical to the 1d tight-binding model. We are

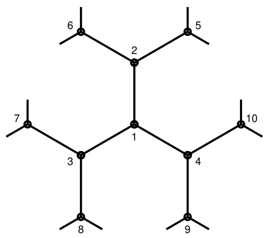

Fig. 4.6. Bethe lattice for $Z = 3$ nearest neighbors.

again interested in the local Green's function

$$g_{ii}^{\sigma}(\omega) = -\frac{1}{\pi}\left\langle\!\left\langle a_{i\sigma}; a_{i\sigma}^{\dagger}\right\rangle\!\right\rangle_{w}.$$

The hamiltonian is identical to that of the tight-binding model with the modified meaning of nearest neighbor sites. If all on-site energies are identical, the Greens function is independent of the site index i. We enumerate the sites as depicted in Fig.4.6 and start the Lanczos procedure with $|\varphi_0\rangle = |1\rangle$, where again $|i\rangle = a_{i\uparrow}^{\dagger}$. The Hamiltonian moves the particle from site 1 to its Z nearest neighbors, hence $|\varphi_1\rangle$ is a homogeneous superposition of the basis vectors $|j\rangle$ for the Z nearest neighbor sites. These sites $\{2, 3, 4\}$ form the 'shell' of sites which have Manhattan distance 1 from the origin. Accordingly, $k_1^2 = Zt^2$. Application of H on $|\varphi_1\rangle$ moves the particle to the next 'shell' composed of the $Z-1$ nearest neighbors of each of the sites of shell '2'. These sites have Manhattan distance '2' from the origin. The sites of the second shell are $\{5, 6, 7, 8, 9, 10\}$. Contribution of the hopping processes to inner shells are eliminated by the orthogonality constraint. The matrix element $k_2^2 = N(2)/N(1)$, where $N(i)$ is the number of sites of shell 'i'. These numbers are readily computed by the recursion relation $N(i+1) = N(i) * (Z-1)$, as each site of shell 'i' has $Z-1$ nearest neighbors in shell $i+1$. So the matrix elements of the hamiltonian in the Lanczos basis are

$$\begin{aligned} k_1^2 &= Zt^2 \\ k_i^2 &= (Z-1)t^2; \qquad \forall i > 1 \\ \epsilon_i &= 0 \; . \end{aligned}$$

The continued fraction for the local Greens function is therefore

$$g_{ii}(\omega) = \cfrac{1}{\omega - \cfrac{Zt^2}{\omega - \cfrac{(Z-1)t^2}{\omega - \cfrac{(Z-1)t^2}{\omega - \cdots}}}} \; .$$

We see that the special case $Z = 2$ is indeed identical to the 1-d result derived before. We can even use the same trick to determine the Greens function.

$$\begin{aligned} g &= \frac{1}{\omega - Zt^2 G} \\ G &= \frac{1}{\omega - KG} \; , \end{aligned}$$

with $K = (Z-1)t^2$. The solution yields

$$G = \frac{\omega \pm \sqrt{\omega^2 - 4K}}{2K}$$

and

$$g = \frac{2}{\omega \frac{(Z-2)}{Z-1} + \frac{Z}{Z-1}\sqrt{\omega^2 - 4t^2(Z-1)}} \; ,$$

where the unphysical solution has been discarded We will compute the DOS for an infinite-dimensional lattice, i.e. for $Z = \infty$. In this case the greens function simplifies further

$$g = \frac{2}{\omega + \sqrt{\omega^2 - 4t^2 Z}}$$

to the so called Hubbard Green's function. The imaginary part is finite only for $\omega^2 < t^2 Z$. In this case the density of states is

$$\rho(\omega) = \frac{\sqrt{4t^2 Z - \omega^2}}{2\pi t^2 Z} \; .$$

In order to get physically meaningful results in the $d - \infty$ limit, we introduce the scaling $t = t^*/\sqrt{Z}$ for the hopping matrix element, yielding a finite limiting DOS

$$\rho(\omega) = \frac{\sqrt{4t^{*2} - \omega^2}}{2\pi t^{*2}} \; .$$

4.3 Davidson–Liu Algorithm

Like the Lanczos method, the Davidson-Liu algorithm was devised for the computation of the lowest few eigenvalues and eigenvectors of huge matrices $\mathbb{H}$. It also relies heavily on sparsity of the matrix. The eigenvalue problem, which we want to solve for the lowest eigenvalues, shall be denoted by

$$\mathbb{H}\,\mathbf{c}_k = \lambda_k\,\mathbf{c}_k \;, \tag{4.55}$$

where $\mathbf{c}_k$ are the eigenvectors and λ_k the eigenvalues. We assume that the eigenvalues λ_k are sorted in ascending order.

The vital points of the Lanczos approach also apply to the Davidson–Liu algorithm:

- The physically most relevant basis vectors are constructed, in which the matrix elements of the Hamilton and the eigenvectors are expanded. The basis vectors are denoted by $\{\mathbf{b}_p\}, \quad p = 1, 2, \ldots, P$.
- The number P of basis vectors, required for a decent approximation as far as eigenvalues and eigenvectors are concerned, is considerably smaller than the dimension N of the matrix $\mathbb{H}$ to be diagonalized.
- The diagonalization of the resulting $P \times P$ matrix $\tilde{K}$ can be achieved by standard eigenvalue routines.
- The eigenvectors follow from the

$$\mathbf{x}_k = \sum_{p=1}^{P} a_{pk}\mathbf{b}_p \tag{4.56}$$

Nevertheless, if this intermediate set of vectors $\mathbf{b}_p$ is chosen in a convenient manner, the expansion

will converge to the real eigenvector $\mathbf{c}_k$ even if $P \ll N$. Of course, this is only true if the a_{pk} are chosen properly. To this end, we organize the vectors $\mathbf{b}_k$ as the columns of matrix $\mathbb{B}$ and the expansion coefficients in a column vector $\mathbf{a}_k$. Then the variational approximation to the solution of the eigenvalue problem in the subspace spanned by $\{\mathbf{b}_k\}$ becomes

$$\mathbb{B}^\dagger\,\mathbb{H}\,\mathbb{B}\,\mathbf{a}_k = \mu_k^P\,\mathbb{B}^\dagger\,\mathbb{B}\,\mathbf{a}_k \;, \qquad k = 1, \ldots, P \;. \tag{4.57}$$

If also numbered in increasing order, the eigenvalues μ_k^P are approximations of the real eigenvalues λ_k. Furthermore, by the Hylleraas–Undheim–MacDonald variational principle, we have

$$\lambda_k \le \mu_k^P \;, \qquad k = 1, \ldots, P \;. \tag{4.58}$$

If we add one further vector to the set of $\{\mathbf{b}_k\}$, then the same principle states

$$\mu_k^{P+1} \le \mu_k^P \;, \qquad k = 1, \ldots, P \;. \tag{4.59}$$

These observations show that a general strategy is possible in which the eigenvalues $\{\mu_k^P\}$ with $k = 1, \ldots, K$ and $p = K, K+1, \ldots$ form a momotonic non–increasing sequence that converges to the exact eigenvalues $\{\lambda_k\}$ for $k = 1, \ldots, K$. In what follows, we will outline such a strategy.

First we introduce a set of K vectors $\mathbf{b}_k$ that spans a K–dimensional sub–space of the original Hilbert space. These vectors shall have a significant overlap with the lowest eigenstates and may, in some cases, be inferred from physical considerations A common method of generating this *initial guess* would be by diagonalization of a small submatrix of $\mathbb{H}$. The simplest alternative would be to choose unit vectors according to the smallest diagonal elements of $\mathbb{H}$. In this sub–space we consider the approximated eigenstates $\mathbf{x}_k$ according to (4.56) and (4.57). Next we try to approximate the error $\boldsymbol{\delta}_k = \mathbf{c}_k - \mathbf{x}_k$. By introducing the residual $\mathbf{r}_k = (\mathbb{H} - \lambda_k \mathbb{I})\, \mathbf{x}_k$ we obtain from the original eigenvalue equation (4.55)

$$(\mathbb{H} - \lambda_k\, \mathbb{I})\, \boldsymbol{\delta}_k = -\mathbf{r}_k \; . \tag{4.60}$$

By solving this equation, we can calculate the corrections $\boldsymbol{\delta}_k$ to each approximated eigenvector. In order to take advantage of this formula, however, we first need the exact eigenvalues λ_k that are, of course, not at our disposal. Thus we approximate them by the Rayleigh quotient

$$\rho_k = \frac{\mathbf{x}_k^\dagger \mathbb{H}\, \mathbf{x}_k}{\mathbf{x}_k^\dagger\, \mathbf{x}_k} \; ,$$

that is in practice close to the actual eigenvalue even if $\mathbf{x}_k$ is only a coarse approximation of the true eigenvector $\mathbf{c}_k$. Second, the inversion of the huge matrix $\mathbb{H} - \rho_k\, \mathbb{I}$ is not possible and we approximate this matrix by $\mathbb{D} - \rho_k\, \mathbb{I}$, where $\mathbb{D}$ contains just the diagonal elements of $\mathbb{H}$. Therefore, we obtain the corrections

$$\boldsymbol{\delta}_k \approx -(\mathbb{D} - \rho_k \mathbb{I})^{-1}\, \mathbf{r}_k \; . \tag{4.61}$$

These corrections could be used directly ($\mathbf{c}_k = \mathbf{x}_k + \boldsymbol{\delta}_k$) to obtain a better approximation of the eigenvectors. In practice this does not work very well because of the simplifications made during their calculation. It turns out, however, that the $\boldsymbol{\delta}_k$ are a good choice for the next addition to the set $\{\mathbf{b}\}$. Therefore, we add $\boldsymbol{\delta}_k$ to $\{\mathbf{b}\}$ and re–iterate the procedure. This is done until no noticeable corrections (residuals $\mathbf{r}_k$) are observed any more.

Summarizing, we can say that the Davidson–Liu algorithm comprises the following steps:

1. Create a list $j(p), p = 1, \ldots, K$ of the indices of the K lowest diagonal elements of the Hamiltonian $\mathbb{H}$. Initialize the vectors $\mathbf{b}^p$ as unit vectors $b_i^p = \delta_{j(p),i}$. Summarize them to the columns of the matrix $\mathbb{B}$. Initialize $\mathbf{h}_p$ as $\mathbf{h}_p = \mathbb{H}\, \mathbf{u}_p$ (p–th column of the matrix $\mathbb{H}$). Calculate $(\mathbb{B}^\dagger \mathbb{H}\, \mathbb{B})_{pq} = H_{j(p)j(q)}$.

2. Get eigenvalues μ and eigenvectors $\mathbf{a}$ of $\mathbb{B}^\dagger \mathbb{H}\,\mathbb{B}$.
3. Calculate the residuals $\mathbf{r}_k = \sum(\mathbf{h}_p - \mu_k \mathbf{b}_p)\, a_{pk}$.
4. Test for convergence and stop if all residuals $\mathbf{r}_k$ are small enough. Else select up to Q residuals of maximum norm for improvement.
5. Check if the addition of Q vectors to the set $\{\mathbf{b}\}$ will exceed the limits imposed on the size of this set. If no, skip the next two items.
6. Replace the set $\{\mathbf{b}\}$ by the lowest approximated eigenvectors $\{\mathbf{x}_k^p, k = 1, \ldots, K\}$. If there is still space, also retain the lowest unconverged vectors of the previous iteration, i.e. $\{\mathbf{x}_k^{p-1}, k = 1, \ldots\}$ orthogonalized to $\{\mathbf{x}_k^p, k = 1, \ldots, K\}$.
7. Expand the new set $\{\mathbf{b}^{new}\}$ in terms of linear combinations of the old one $\{\mathbf{b}^{old}\}$: $\mathbf{b}_p^{new} = A_{pl}\, \mathbf{b}_l^{old}$. Calculate $\mathbf{h}_p^{new} = \mathbb{H}\mathbf{b}_p^{new} = \sum A_{pl}\, \mathbf{h}_l^{old}$. Replace $\mathbb{B}^\dagger \mathbb{H}\,\mathbb{B}$ by the new $\mathbf{b}_p^{new\dagger} \mathbf{h}_q^{new}$.
8. Calculate the corrections $\boldsymbol{\delta}_k$ for all Q chosen vectors: $\delta_{ik} = {d_{ik}}^{-1}\, r_{ik}$ with $d_{ik} = D_{ii} - \mu_k$ if $|D_{ii} - \mu_k| > \varepsilon > 0$ and $d_{ik} = \varepsilon \,\mathrm{sign}\,(D_{ii} - \mu_k)$ otherwise. Orthogonalize this set of $\boldsymbol{\delta}_k$ to $\{\mathbf{b}\}$ and to each other and append the result to $\{\mathbf{b}\}$.
9. For all $\mathbf{b}$ added in the previous step, form $\mathbf{h} = \mathbb{H}\,\mathbf{b}$ and append these to the set $\{\mathbf{h}\}$. Complete $\mathbb{B}^\dagger \mathbb{H}\,\mathbb{B}$ by the additional rows and columns formed from the added vectors $\mathbf{b}$ and from all of the vectors $\mathbf{h}$.
10. Continue at step 2.

Of course, a good choice of the initial sub–space $\{\mathbf{b}\}$ accelerates the convergence of the algorithm. If the ground state of $\mathbb{H}$ happens to be orthogonal to this space, the algorithm will fail to calculate it.

Steps 5 and 6 deserve additional comments: Without them, the dimension of the sub–space would grow at each iteration by Q. This has the consequence that the practical limits on the size of this space are reached after a few iterations although no convergence of the eigenvectors and eigenvalues has yet been achieved. Thus, as soon as this happens, we try to eliminate the least important part of this space. In principle this is done by keeping the eigenspaces of the lowest few eigenvalues of the last iteration.

4.3.1 Alternative Approach

In what follows, we want to present a derivation of the Davidson–Liu algorithm in the context of Brillouin Wigner perturbation theory. As usual in the framework of perturbation theory, we split the Hamiltonian $\hat{H}$ in two parts,

$$\hat{H} = \hat{H}_0 + \hat{H}_1 \; . \tag{4.62}$$

and assume that we can solve the eigenvalue problem for the operator $\hat{H}_0$ explicitly. Therefore we dispose of all eigenvalues E_n^0 and corresponding eigenvectors $\left|\Phi_n^0\right\rangle$,

$$\hat{H}_0 \left|\Phi_n^0\right\rangle = E_n^0 \left|\Phi_n^0\right\rangle \; . \tag{4.63}$$

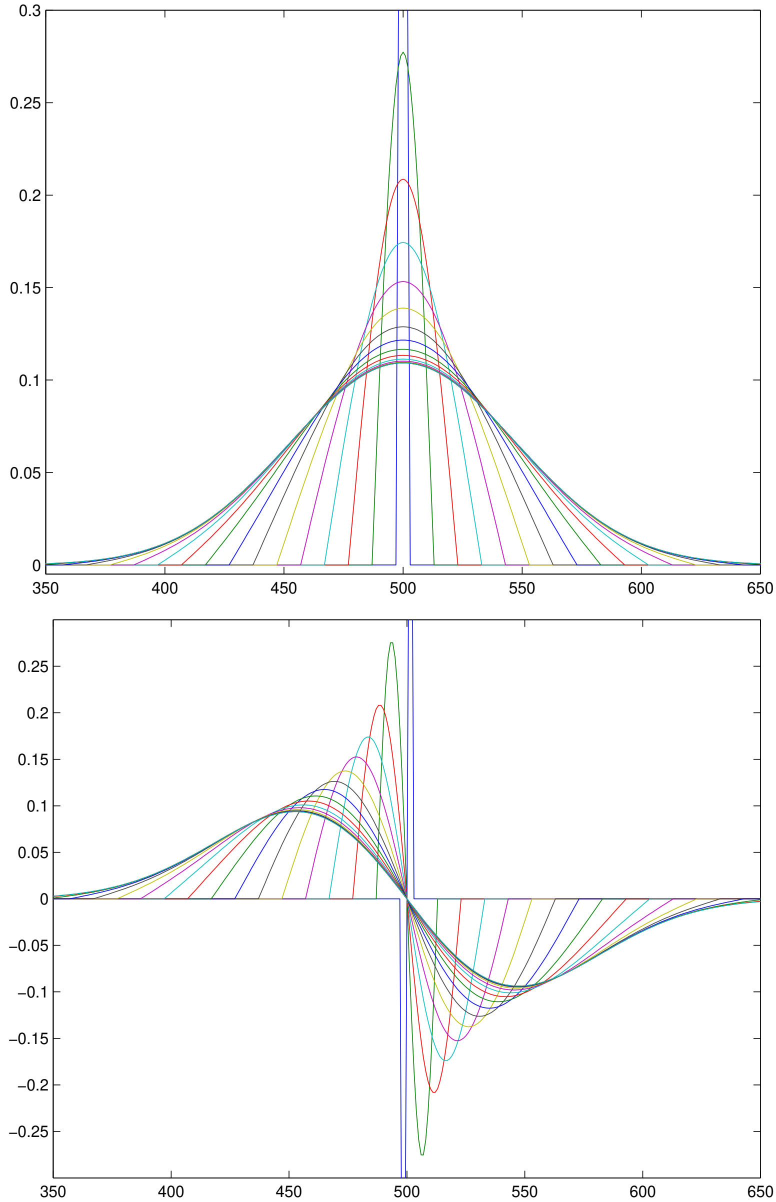
0.3
0.25
0.2
0.15
0.1
0.05
0
350
400
450
500
550
600
650
0.25
0.2
0.15
0.1
0.05
0
−0.05
−0.1
−0.15
−0.2
−0.25
350
400
450
500
550
600
650

Now we want to calculate the n-th eigenvector $|\Phi_n\rangle$ of the perturbed problem. The appropriate formula (Brillouin Wigner) reads

$$|\Phi_n\rangle = \left(\hat{I} - \left(E_n - \hat{H}_0\right)^{-1} \hat{Q}\,\hat{H}_1\right)^{-1} \left|\Phi_n^0\right\rangle . \tag{4.64}$$

As a typical feature of the Brillouin Wigner approach, the full eigenvalue E_n appears in the formula. The operator $\hat{Q}$ projects on the orthogonal complement of the space spanned by $\left|\Phi_n^0\right\rangle$. Up to the first order, we can express the outer inversion as

$$\begin{aligned} |\Phi_n\rangle &\approx \left(\hat{I} + \left(E_n - \hat{H}_0\right)^{-1} \hat{Q}\,\hat{H}_1\right) \left|\Phi_n^0\right\rangle \\ &= \left|\Phi_n^0\right\rangle + \left(E_n - \hat{H}_0\right)^{-1} \hat{Q}\,\hat{H}_1 \left|\Phi_n^0\right\rangle \\ &= \left|\Phi_n^0\right\rangle + \left(E_n - \hat{H}_0\right)^{-1} \hat{Q}\,\hat{H} \left|\Phi_n^0\right\rangle . \end{aligned} \tag{4.65}$$

The substitution of $\hat{H}_1$ by the entire operator $\hat{H} = \hat{H}_0 + \hat{H}_1$ is possible because $\hat{H}_0 \left|\Phi_n^0\right\rangle = E_n^0 \left|\Phi_n^0\right\rangle$ which is subsequently projected out by $\hat{Q}$.

For the derivation of the Davidson–Liu algorithm, we are interested in the perturbation corrections orthogonal to the unperturbed eigenvector $\left|\Phi_n^0\right\rangle$. Therefore, we apply the projector $\hat{Q}$ to (4.65) and obtain

$$\begin{aligned} \left|\Phi_n^1\right\rangle &\equiv \hat{Q} \left|\Phi_n^0\right\rangle \\ &= \hat{Q} \left(E_n - \hat{H}_0\right)^{-1} \hat{Q}\,\hat{H} \left|\Phi_n^0\right\rangle . \end{aligned} \tag{4.66}$$

Now we take advantage of the explicit form of the projector, i.e. $\hat{Q} = \hat{I} - \left|\Phi_n^0\right\rangle\left\langle\Phi_n^0\right|$. This yields the expression

$$\hat{Q}\,\hat{H} \left|\Phi_n^0\right\rangle = \hat{H} \left|\Phi_n^0\right\rangle - \left\langle\Phi_n^0\middle|\hat{H}\middle|\Phi_n^0\right\rangle \left|\Phi_n^0\right\rangle\!\left|\Phi_n^0\right\rangle , \tag{4.67}$$

which can, in turn, be inserted into (4.66). Consequently, we obtain

$$\begin{aligned} \left|\Phi_n^1\right\rangle &= \hat{Q} \left(E_n - \hat{H}_0\right)^{-1} \left|\Phi_n^0\right\rangle - \left\langle\Phi_n^0\middle|\hat{H}\middle|\Phi_n^0\right\rangle \hat{Q} \left(E_n - \hat{H}_0\right)^{-1} \left|\Phi_n^0\right\rangle \\ &= \hat{Q} \left(E_n - \hat{H}_0\right)^{-1} \left|\Phi_n^0\right\rangle - \left\langle\Phi_n^0\middle|\hat{H}\middle|\Phi_n^0\right\rangle \hat{Q}\,\frac{1}{E_n - E_n^0} \left|\Phi_n^0\right\rangle . \end{aligned} \tag{4.68}$$

Since $\hat{Q} \left|\Phi_n^0\right\rangle = 0$, the second term of (4.68) vanishes and we are led to the simple expression

$$\left|\Phi_n^1\right\rangle = \hat{Q} \left(E_n - \hat{H}_0\right)^{-1} \left|\Phi_n^0\right\rangle . \tag{4.69}$$

Now we have to resort to another approximation, because the energies of the full, perturbed problem are not at our disposal. By substituting them with the expectation value of $\hat{H}$ in the state $\left|\Phi_n^0\right\rangle$, we end up with

$$\left|\Phi_n^1\right\rangle = \hat{Q}\left(\left\langle\Phi_n^0\right|\hat{H}\left|\Phi_n^0\right\rangle - \hat{H}_0\right)^{-1}\hat{H}\left|\Phi_n^0\right\rangle . \tag{4.70}$$

Upon identifying $\hat{H}_0$ with the diagonal part of the potential and $\hat{H}_1$ with the rest of the Hamiltonian, this last equation corresponds exactly to the Davidson–Liu formula. Therefore, up to first order Brillouin Wigner perturbation theory, the corrections on $\left|\Phi_n^0\right\rangle$ are to be made in direction of $\left|\Phi_n^1\right\rangle$. The actual weight of these corrections can be optimized by diagonalizing the Hamiltonian $\hat{H}$ in the subspace $\{\left|\Phi_n^0\right\rangle, \left|\Phi_n^1\right\rangle\}$.

4.4 The Kernel-Polynomial Method

Many physical properties, such as the mean energy, free energy and entropy, can be determined directly from the density of states $\rho(\omega)$ (DOS). It can be computed directly by several numerical techniques,e.g. by Monte-Carlo-techniques. Here we will present an approach which deduces the density of states from its moments

$$\mu_m = \int \rho(\omega)\, \omega^m \, d\omega \; .$$

The moments are accessible by an iteration procedure which is closely related to the Lanczos scheme. If all μ_m are known then $\rho(\omega)$ can be reconstructed exactly. There are two drawbacks to the straight-forward application of this idea. Firstly, it is numerically instable beyond $m = O(10)$, secondly in practice only a finite number of moments will be available which results in Gibbs-type of oscillations in the reconstructed density of states.

Silver and Röder [15, 16] proposed the so-called *Kernel Polynomial Method* (KPM) in order to overcome both shortcomings. The numerical stability can be improved by using orthogonal polynomials, instead of the linearly dependent powers ω^n. Best suited are *Chebyshev polynomials* T_k, which avoids accumulation of numerical roundoff errors and have optimal convergence properties. For details see [17]. The problem of Gibbs-oscillations is already strongly reduced by Chebyshev polynomials and can be decreased beyond that upon using appropriate broadening functions *kernels.* These topics will be discussed in the sequel.

4.4.1 Chebyshev Polynomials

To begin with, we briefly outline the properties of Chebyshev polynomials in so far as they are utilized in the ensuing discussion. Chebyshev polynomials are defined recursively by

$$\begin{aligned} T_k : [-1,1] &\rightarrow [-1,1] \\ T_0(x) &= 1 \\ T_1(x) &= x \\ T_{n+1}(x) &= 2\,x\,T_n(x) - T_{n-1}(x) \; . \end{aligned} \tag{4.71}$$

The first six polynomials $(T_0 \ldots T_5)$ are sketched in Fig. 4.7. Chebyshev polynomials have the boundary values $|T_n(\pm 1)| = 1$. The orthogonality relation reads

$$\int_{-1}^{1} w(x)\, T_n(x)\, T_m(x)\, dx = \frac{\pi}{2}\, \delta_{n,m}\, (\delta_{n,0} + 1) \; . \tag{4.72}$$

It is based on the weight function

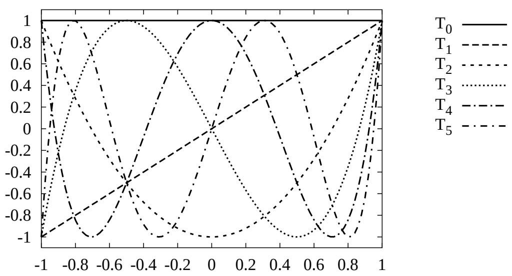

Fig. 4.7. First six Chebyshev polynomials

$$w(x) = \frac{1}{\sqrt{1-x^2}} \; . \tag{4.73}$$

Chebyshev polynomials are intimately related to trigonometric functions via a variable transformation

$$\begin{aligned} \varphi &= \arccos(x) \\ d\varphi &= w(x)\; dx \; . \end{aligned} \tag{4.74}$$

In fact, they can be written as

$$T_n(x) = \cos(n \; \arccos(x)) = \cos(n\varphi) \; , \tag{4.75}$$

as can be shown by induction ($T_0(x) = \cos(0 \arccos(x)) = 0, T_1(x) = \cos(1 \arccos(x)) = x$) using the recursion relation (4.72). The orthogonality relation (4.72) immediately follows from the orthogonality of the cosine functions on the interval $[0, 2\pi)$.

$$\int_{-1}^{1} w(x)\; T_n(x)\; T_m(x)\; dx = \int_{0}^{2\pi} \cos(n\varphi)\; \cos(m\varphi)\; d\varphi = \frac{\pi}{2}\; \delta_{n,m}\; (\delta_{n,0}+1) \; .$$

From (4.75) it is apparent that $|T_n(x)| \leq 1$. Moreover (4.74) yields the useful relation $T_{2n}(x) = \cos(2n\varphi) = 2\; \cos^2(n\varphi) - 1$. This and a similar consideration yields

$$\begin{aligned} T_{2n}(x) &= 2\, T_n(x)\, T_n(x) - T_0(x) \\ T_{2n+1}(x) &= 2\, T_n(x)\, T_{n+1}(x) - T_1(x) \; . \end{aligned} \tag{4.76}$$

These equations will be utilized to derive the moments of order $M+1, \ldots, 2M$ from those of the order $1, \ldots, M$. By virtue of the completeness of the Chebyshev polynomials, any real-valued function $f(x)$ defined for $[-1, 1]$ can be expanded in terms of $T_n(x)$

$$f(x) = w(x) \left(\mu_0 T_0(x) + 2 \sum_{n=1}^{\infty} \mu_n \, T_n(x) \right) \; . \tag{4.77}$$

The coefficients follow from the orthogonality relation (4.72)

$$\mu_n = \frac{1}{\pi} \int_{-1}^{1} f(x)\, T_n(x)\, dx \; . \tag{4.78}$$

Alternatively, one can eliminate the factor $\omega(x)$ from (4.76) and insert it into the integral (4.72) instead. For our purposes, this approach is less useful. In order to obtain a trigonometric representation, we resort to the independent variable $\varphi = \arccos(x)$. Upon absorbing the inverse weight into the definition of the transformed function

$$\tilde{f}(\varphi) \overset{\text{def}}{=} f(\cos(\varphi))|\sin(\varphi)| = f(x)\sqrt{1-x^2} \; ,$$

we obtain from (4.75) and (4.77)

$$\tilde{f}(\varphi) = \mu_0 + 2\sum_{m=1}^{\infty} \mu_m \cos(m\varphi) \tag{4.79}$$

whereas (4.78) can be written as

$$\mu_n = \frac{1}{\pi} \int_{0}^{\pi} \tilde{f}(\varphi)\, \cos(n\varphi)\, d\varphi \; . \tag{4.80}$$

Up to now, $\tilde{f}(\varphi)$ is defined for $\varphi \in [0,\pi]$. We extend the definition to $[0,2\pi]$ by demanding

$$\tilde{f}(\varphi) \overset{\text{def}}{=} \tilde{f}(2\pi - \varphi) \quad \text{for all } \varphi \in [\pi, 2\pi] \; .$$

4.4.2 Expansion of the density of states

In order to expand the density of states in Chebyshev polynomials, we first transform the spectrum σ of the underlying Hamiltonian $\hat{H}$ into the interval $[-1,1]$ by the linear transformation

$$\tilde{\hat{H}} = a \cdot \hat{H} + b \; , \tag{4.81}$$

with modified eigenvalues $\tilde{\varepsilon}_i = a\; \varepsilon_i + b$. The coefficients a and b are chosen as

$$a = \frac{2}{\varepsilon_N - \varepsilon_0} \; , \quad b = -\frac{\varepsilon_0 + \varepsilon_N}{\varepsilon_N - \varepsilon_0} \qquad \text{if } \sigma(H) \subset [\varepsilon_0, \varepsilon_N] \; .$$

Estimates for the lower and upper bound, ε_0 and ε_N respectively, are provided by e.g. the Lanczos recursion method. Obviously, the present approach is restricted to systems with a bounded spectrum. This poses no real restriction, since most finite size systems, addressed by numerical techniques, fulfill the requirements. In other cases one can invoke adequate nonlinear transformations to map the spectrum to the interval $[-1, 1]$. The transformed density of states is given by

$$\tilde{\rho}(\varepsilon) = \frac{1}{N} \sum_{i=1}^{N} \delta(\varepsilon - \tilde{\varepsilon}_i) \ . \tag{4.82}$$

We expansion $\tilde{\rho}(x)$ into Chebyshev polynomials

$$\tilde{\rho}(\varepsilon) = w(\varepsilon) \left(\mu_0 T_0(\varepsilon) + 2 \sum_{n=1}^{\infty} \mu_n \, T_n(\varepsilon) \right) \ . \tag{4.83}$$

The original density of states is obtained by the inverse transformation

$$\rho(\varepsilon) = a \cdot \tilde{\rho}(a\,\varepsilon + b) \ .$$

So far we have merely expanded the DOS in terms of Chebyshev polynomials. Next we discuss how to derive the corresponding coefficients.

4.4.3 Chebyshev Coefficients

Inserting the specific form (4.82) of the density of states into the expression (4.78) for the Chebyshev coefficients yields

$$\begin{aligned} \mu_m &= \frac{1}{\pi} \int \tilde{\rho}(\varepsilon)\, T_m(\varepsilon)\, d\varepsilon = \frac{1}{\pi} \frac{1}{N} \sum_{i=1}^{N} \underbrace{\int \delta(\varepsilon - \tilde{\varepsilon}_i)\, T_m(\varepsilon)\, d\varepsilon}_{T_m(\tilde{\varepsilon}_i)} \\ &= \frac{1}{\pi} \frac{1}{N} \sum_{i=1}^{N} T_m(\tilde{\varepsilon}_i) \ . \end{aligned} \tag{4.84}$$

So far it looks as if this approach leads nowhere, since we still need the eigenvalues of the Hamiltonian in order to compute the Chebyshev coefficients. However, the expression can be cast into a numerically tractable form upon utilizing the eigenvalue equation $\tilde{\hat{H}}|\psi_i\rangle = \tilde{\varepsilon}_i|\psi_i\rangle$

$$\mu_m = \frac{1}{\pi} \frac{1}{N} \sum_{i=1}^{N} \langle \psi_i | T_m(\tilde{\hat{H}}) | \psi_i \rangle = \frac{1}{\pi} \frac{1}{N} \ \mathrm{tr} \left(T_m(\tilde{\hat{H}}) \right) \ . \tag{4.85}$$

The normalization of the DOS determines the zeroth moment $\mu_0 = 1/\pi$. The resulting trace is invariant under changes of the basis so that we need neither the eigenvalues nor eigenvectors anymore. Before we continue with the determination of the Chebyshev coefficients, we discuss a stochastic technique to evaluate the trace of an operator.

4.4.4 Stochastic evaluation of the trace

Although the evaluation of the trace of a matrix is a most elementary operation, the straight forward evaluation is still far too expensive in the present context, since we need the trace of $T_m(\tilde{\hat{H}})$, which involves the m-th power of $\tilde{\hat{H}}$. The trace can instead be evaluated via expectation values in suitably chosen random states $|\Phi_\nu\rangle$

$$T = \frac{1}{L} \sum_{\nu=1}^{L} \langle \Phi_\nu | \, \hat{O} \, | \Phi_\nu \rangle \; . \tag{4.86}$$

In order to prove (4.86) we expand the random vectors

$$|\Phi_\nu\rangle = \sum_{i=1}^{N} c_i^{(\nu)} |\varphi_i\rangle \tag{4.87}$$

in a set of orthonormal basis vectors $|\varphi_i\rangle$, in which the matrix elements of the Hamiltonian can be computed efficiently The stochastic expression for the trace reads

$$T = \frac{1}{L} \sum_{\nu=1}^{L} \sum_{i,j} c_i^{(\nu)} \, c_j^{(\nu)} \langle \varphi_i | \, \hat{O} \, | \varphi_j \rangle \; . \tag{4.88}$$

Now we will discuss under which circumstances T is an unbiased estimator for the trace. The expectation value of T is given by

$$E(T) = \frac{1}{L} \sum_{\nu=1}^{L} \sum_{i,j} E\Big(c_i^{(\nu)} \, c_j^{(\nu)} \Big) O_{ij} \; , \tag{4.89}$$

with $O_{ij} = \langle \varphi_i | \, \hat{O} \, | \varphi_j \rangle$. The estimator T is apparently unbiased if

$$E\Big(c_i^{(\nu)} \, c_j^{(\nu)} \Big) = \delta_{ij} \; . \tag{4.90}$$

In addition we demand that $c_i^{(\nu)}$ are iid random numbers with zero mean, i.e.

$$\begin{aligned} E(c_i^{(\nu)}) &= 0 \\ E\Big(c_i^{(\nu)} \, c_j^{(\nu')} \Big) &= \delta_{ij} \; \delta_{\nu\nu'} \; . \end{aligned} \tag{4.91}$$

Next we turn to the question of efficiency. To this end we compute the variance of T

$$
\begin{aligned}
E(T^2) &= E\left(\left[\frac{1}{L}\sum_{\nu=1}^{L}\langle\Phi_\nu|\hat{O}|\Phi_\nu\rangle\right]^2\right) \\
&= E\left(\frac{1}{L^2}\sum_{\nu,\nu'}\langle\Phi_\nu|\hat{O}|\Phi_\nu\rangle\langle\psi_{\nu'}|\hat{O}|\psi_{\nu'}\rangle\right) \\
&= \frac{1}{L^2}\sum_{\nu,\nu'}\sum_{i,j,i',j'} E\Big(c_i^{(\nu)}\,c_j^{(\nu)}\,c_{i'}^{(\nu')}\,c_{j'}^{(\nu')}\Big)\,O_{ij}\,O_{i'j'}\ .
\end{aligned}
\tag{4.92}
$$

We split the sum into

$$
\begin{aligned}
E(T^2) = &\overbrace{\frac{1}{L^2}\sum_{\nu\neq\nu'}\sum_{i,j,i',j'} E\Big(c_i^{(\nu)}\,c_j^{(\nu)}\,c_{i'}^{(\nu')}\,c_{j'}^{(\nu')}\Big)\,O_{ij}\,O_{i'j'}}^{E_1} \\
&+\underbrace{\frac{1}{L^2}\sum_{\nu}\sum_{i,j,i',j'} E\Big(c_i^{(\nu)}\,c_j^{(\nu)}\,c_{i'}^{(\nu)}\,c_{j'}^{(\nu)}\Big)\,O_{ij}\,O_{i'j'}}_{E_2}\ .
\end{aligned}
$$

By virtue of (4.91), t he first sum simplifies to

$$
E_1 = \frac{L-1}{L}\ \mathrm{tr}(O)^2\ .
$$

In the second sum the upper index can be suppressed as we assume iid random variables $c_i^{(\nu)}$, i.e.

$$
E_2 = \frac{1}{L}\sum_{i,j,i',j'} E\Big(c_i\,c_j\,c_{i'}\,c_{j'}\Big)\,O_{ij}\,O_{i'j'}
$$

Due to the vanishing mean, $E(c_i) = 0$, finite contributions to the sum require that the indices i, j, i', j' show up in pairs or even quadruples. The following table summarizes the possible cases which contribute to the sum

no.	Conditions	Expectation
1	$i = j \,\wedge\, i' = j' \,\wedge\, i \neq i'$	$E(c_i^2)E(c_i'^2) = 1$
2	$i = i' \,\wedge\, j = j' \,\wedge\, i \neq j$	$E(c_i^2)E(c_j^2) = 1$
3	$i = j' \,\wedge\, j = i' \,\wedge\, i \neq j$	$E(c_i^2)E(c_j^2) = 1$
4	$i = j = i' = j'$	$E(c_i^4) = E(c^4)$

These cases lead to

$$
\begin{aligned}
E_2 &= \frac{1}{L} \sum_{iji'j'} E\left(c_i\, c_j\, c_{i'}\, c_{j'}\right)\, O_{ij}\, O_{i'j'} \\
&= \frac{1}{L} \left(\sum_{ii'} O_{ii} O_{i'i'} - \sum_i O_{ii} O_{ii} \right) + \frac{1}{L} \left(\sum_{ij} O_{ij} O_{ij} - \sum_i O_{ii} O_{ii} \right) \\
&+ \frac{1}{L} \left(\sum_{ij} O_{ij} O_{ji} - \sum_i O_{ii} O_{ii} \right) + \frac{E(c^4)}{L} \sum_i O_{ii} O_{ii} \\
&= \frac{1}{L}\ \mathrm{tr}(O)^2 + \frac{2}{L}\ \mathrm{tr}(O^2) + \frac{E(c^4) - 3}{L} \sum_i O_{ii}^2 \, .
\end{aligned}
$$

We finally obtain

$$
\mathrm{var}(T) = \frac{2}{L}\ \mathrm{tr}(O^2) + \frac{E(c^4) - 3}{L} \sum_i O_{ii}^2 \, .
$$

Of practical importance are the following distributions:

$$
\begin{aligned}
\text{Normal:} &\quad p(c) = \mathcal{N}(\mu = 0, \sigma = 1), && \text{with} \quad E(c^4) = 3. \\
\text{Uniform:} &\quad p(c) = \frac{1}{2\sqrt{3}}\, \theta(|c| \le \sqrt{3}), && \text{with} \quad E(c^4) = 1.8. \\
\text{Delta:} &\quad p(c) = \frac{1}{2} \Big(\delta(x-1) + \delta(x+1) \Big), && \text{with} \quad E(c^4) = 1.
\end{aligned}
$$

Apparently, the last choice is the one which minimizes $var(T)$ and presents the efficient estimator. If the Hamilton matrix O_{ij} is sparse with $O(1)$ non-zero elements per row like in the many-body models, discussed in the introductory chapter, then

$$
\mathrm{var}(T) = \frac{C\, N}{L} \, , \tag{4.93}
$$

with C being a constant independent of N and L. The trace itself, i.e. $E(T)$, is of order $O(N)$. Consequently, the relative statistical error is $O(1/\sqrt{NL})$. We therefore have the remarkable fact that the statistical error in the stochastic evaluation of the trace decreases with the dimension of the problem.

4.4.5 Calculation of the Moments $\boldsymbol{\mu_m}$

We paved the way to finalize the formalism for the Chebyshev moments, for which we employ the estimates $\bar{\mu}_m$

$$
\bar{\mu}_m = \frac{1}{\pi} \frac{1}{N} \frac{1}{L} \sum_{\nu=1}^{L} \underbrace{\langle \Phi_\nu | T_m(\tilde{\hat{H}}) | \Phi_\nu \rangle}_{\stackrel{\mathrm{def}}{=} \mu_m^{(\nu)}} \, . \tag{4.94}
$$

Why have we gained anything? After all, the expression looks identical to the one we started off with. The crucial difference is, that we do not have to sum over all N vectors of a complete basis any longer. Instead, we sum over a much smaller number ($L \ll N$) of random vectors.

The ensuing calculation has to be done separately for every random vector $|\Phi_\nu\rangle$, or rather for random vector of coefficients $\boldsymbol{c}^{(\nu)}$. The recursion formula (4.72) can readily be generalized to operator-valued Chebyshev polynomials

$$T_{m+1}(\tilde{\hat{H}}) = 2\,\tilde{\hat{H}}\,T_m(\tilde{\hat{H}}) - T_{m-1}(\tilde{\hat{H}}) \; . \tag{4.95}$$

Application to $|\Phi_\nu\rangle$ yields the recursion

$$T_{m+1}(\tilde{\hat{H}})\,|\Phi_\nu\rangle = 2\,\tilde{\hat{H}}\,T_m(\tilde{\hat{H}})\,|\Phi_\nu\rangle - T_{m-1}(\tilde{\hat{H}})\,|\Phi_\nu\rangle \; , \tag{4.96}$$

which resembles already very much the Lanczos procedure. We define new vectors

$$|\chi_m\rangle \stackrel{\text{def}}{=} T_m(\tilde{\hat{H}})\,|\Phi_\nu\rangle \; , \tag{4.97}$$

where we suppress the index ν, which is fixed throughout the following considerations. The first vector $|\chi_0\rangle$ is by definition identical to the random vector $|\Phi_\nu\rangle$. From (4.96) we conclude

$$|\chi_{m+1}\rangle = 2\,\tilde{\hat{H}}\,|\chi_m\rangle \;-\; |\chi_{m-1}\rangle \; . \tag{4.98}$$

Similar to Lanczos, the main part of the prescription is to apply the Hamiltonian to a ket $|\chi_m\rangle$. The contributions $\mu_m^{(\nu)}$ to the Chebyshev moments are obtained upon multiplying (4.97) from the left by $\langle\Phi_\nu|$

$$\mu_m^{(\nu)} = \;\langle\Phi_\nu|\,T_m(\tilde{\hat{H}})\,|\Phi_\nu\rangle = \langle\Phi_\nu\,|\chi_m\,\rangle \; . \tag{4.99}$$

We exploit (4.76) in order to reduce the computational costs

$$\begin{aligned}
\mu_{2m}^{(\nu)} &= 2\langle\Phi_\nu|\,T_m(\tilde{\hat{H}})T_m(\tilde{\hat{H}})\,|\Phi_\nu\rangle - \langle\Phi_\nu|\,T_0(\tilde{\hat{H}})\,|\Phi_\nu\rangle \\
&= 2\langle\chi_m\,|\chi_m\,\rangle - \mu_0^{(\nu)} \\
\mu_{2m-1}^{(\nu)} &= 2\langle\chi_m\,|\chi_{m-1}\,\rangle - \mu_1^{(\nu)}
\end{aligned}$$

We expand all vectors in the basis $\{|\varphi_i\rangle\}$

$$|\chi_m\rangle = \sum_{i=1}^{N} d_{im}\,|\varphi_i\rangle \; .$$

Upon defining the vectors $\boldsymbol{d}_m$, whose elements are d_{im} [1], one obtains

[1] note that $\boldsymbol{d}_0 = \boldsymbol{c}^{(\nu)}$

$$\begin{aligned}
\mu_m^{(\nu)} &= \boldsymbol{d}_0^T \boldsymbol{d}_m \\
\mu_{2m}^{(\nu)} &= \boldsymbol{d}_m^T \boldsymbol{d}_m - \mu_0^{(0)} \\
\mu_{2m-1}^{(\nu)} &= \boldsymbol{d}_m^T \boldsymbol{d}_{m-1} - \mu_1^{(0)} \; .
\end{aligned}$$

Eventually, the algorithm for the computation of the Chebyshev moments reads

---

Algorithm 4.4.1: Chebyshev moments$(\bar{\mu}_m, L, K, N)$

$$\textbf{initialize:} \begin{cases} K &= 2 * [K/2] \\ \bar{\mu}_m &= 0; \quad \text{for } m = 1, \dots, 2K \\ \bar{\mu}_0 &= 1/\pi \end{cases}$$

for $\nu = 1$ **to** L

$$\begin{cases}
\text{RandomVector}(\boldsymbol{c}_1, \dim = N) \\
\boldsymbol{c}_1 = \tilde{H}\, \boldsymbol{c}_0 \\
\bar{\mu}_1 = \bar{\mu}_1 + \boldsymbol{c}_0^T \boldsymbol{c}_1 \\
\textbf{for } m = 2 \textbf{ to } K \\
\quad \begin{cases}
\boldsymbol{c}_m = 2\tilde{H}\, \boldsymbol{c}_{m-1} - \boldsymbol{c}_{m-2} \\
\bar{\mu}_m = \bar{\mu}_m + \boldsymbol{c}_0^T \boldsymbol{c}_m \\
\textbf{if } m > K/2 \\
\quad \textbf{then} \begin{cases} \bar{\mu}_{2m-1} = \bar{\mu}_{2m-1} + \boldsymbol{c}_m^T \boldsymbol{c}_{m-1} \\ \bar{\mu}_{2m} \quad\;\; = \bar{\mu}_{2m} + \boldsymbol{c}_m^T \boldsymbol{c}_m \end{cases}
\end{cases}
\end{cases}$$

$$\begin{aligned}
\bar{\mu}_m &= \bar{\mu}_m / \pi L N; && \text{for } m = 1, \dots, 2K \\
\bar{\mu}_{2m-\alpha} &= 2\bar{\mu}_{2m-\alpha} - \bar{\mu}_\alpha; && \text{for } m = K/2, \dots, K \text{ and } \alpha = 0, 1
\end{aligned}$$

According to (4.85) the zeroth moment is exactly known and is excluded from the stochastic evaluation. The matrix elements of the Hamiltonian are defined by $\tilde{H}_{ij} = \langle \varphi_i | \hat{H} | \varphi_j \rangle$. The operation $2 * [K/2]$ enforces even K.

4.4.6 Corrections of Gibbs oscillations

It is obvious that the above algorithm can only be used to compute a finite, actually a small, number M of Chebyshev moments μ_m. Thus we have to truncate the series (4.77). In the first place this yields the approximation

$$f(x) \approx f^{(K)}(x) = w(x) \Big(\mu_0 + 2 \sum_{m=1}^{M} \mu_m \, T_m(x) \Big) \; . \tag{4.100}$$

The truncation does not only reduce the accuracy of the reconstruction of $\tilde{\rho}(x)$, it also introduces *Gibbs oscillations*, known from the theory of Fourier

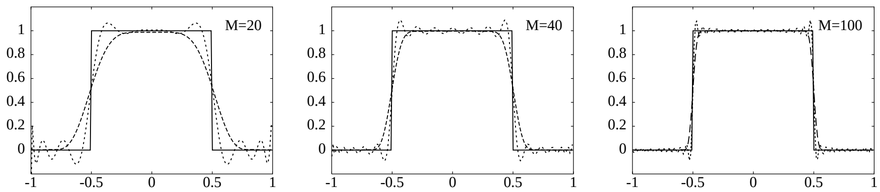

Fig. 4.8. Comparison between the exact shape (solid lines) of the function, reconstruction without (dotted lines) and with (dashed lines) damping factors

transformation. The oscillations are most prominent at sudden changes in the sought-for function. An example is given in Fig. 4.8, where a step function is approximated by a finite Chebyshev series. The results for three different cut-off values M are depicted as dotted lines. The *ringing* is particularly disturbing in densities of states as they might be misinterpreted as elementary excitations of the physical system.

As proposed by Silver and Röder, the Gibbs oscillations can be suppressed by modifying the truncated series. To this end we introduce the weights

$$g_m^{(M)} = \begin{cases} 1 \ldots m \leq M \\ 0 \ldots m > M \end{cases} \tag{4.101}$$

and write the truncated series (4.100) as

$$f^{(M)}(x) = w(x)\Big(\mu_0\, g_0^{(M)} + 2\sum_{m=1}^{\infty} \mu_m\, g_m^{(M)}\, T_m(x)\Big) \ . \tag{4.102}$$

This representation underlines that (4.100) is one ad-hoc choice of truncating the infinite series. The Gibbs oscillations originate from the discontinuity in $g_m^{(M)}$.

The truncation can, however, be chosen differently in order to avoid the discontinuity at $m = M$ and to eliminate the Gibbs oscillations. To this end the coefficients $\tilde{g}_m^{(M)}$ are tailored to vanish continuously at $m = M$.

The relation between the truncated and the damped series (4.102) and the original function, or rather its infinite Chebyshev series (4.77), is a linear transformation. In x-space it is mediated by the *kernel*

$$\delta_K^{(M)}(x,x') \stackrel{\text{def}}{=} \frac{1}{\pi}\left(\tilde{g}_0^{(M)} + 2\sum_{m=1}^{M} \tilde{g}_m^{(M)}\, T_m(x)\, T_m(x')\right) \ . \tag{4.103}$$

The truncated and damped series is obtained by the integral

$$f^{(M)}(x) = \int_{-1}^{1} \delta_K^{(M)}(x,x')\, f(x')\, dx' \ , \tag{4.104}$$

which is proven easily by use of (4.78),

$$
\begin{aligned}
X(x) &\stackrel{\text{def}}{=} \int_{-1}^{1} \delta_K^{(M)}(x, x')\, f(x')\, dx' \\
&= \frac{1}{\pi} \Big(\tilde{g}_0^{(M)} \int_{-1}^{1} f(x')\, dx' + 2 \sum_{m=1}^{M} \tilde{g}_m^{(M)}\, T_m(x) \int_{-1}^{1} T_m(x')\, f(x')\, dx' \Big) \\
&= \tilde{g}_0^{(M)} \mu_0 + 2 \sum_{m=1}^{M} \tilde{g}_m^{(M)}\; T_m(x)\; \mu_m \; .
\end{aligned}
$$

The choice $\tilde{g}_m^{(M)} = 1$ restores the original truncated series (4.100). As already stated above, in the trigonometric representation, the linear transformation turns out to be a convolution. The kernel has the form

$$
\delta_K^{(M)}(\varphi) = \frac{1}{2\pi} \Big(\tilde{g}_0^{(M)} + 2 \sum_{m=1}^{M} \tilde{g}_m^{(M)}\; \cos(m\varphi) \Big) \; , \tag{4.105}
$$

and the convolution reads

$$
\tilde{f}^{(M)}(\varphi) = \int_0^{2\pi} \; \delta_K^{(M)}(\varphi - \varphi')\; \tilde{f}(\varphi')\; d\varphi' \; . \tag{4.106}
$$

The convolution has a very intuitive meaning. Applied to a δ-peak at φ_0, i.e. $\tilde{f}(\varphi') = \delta(\varphi' - \varphi_0)$, the result of the convolution is $\tilde{f}^{(M)}(\varphi) = \delta_K^{(M)}(\varphi - \varphi_0)$. Therefore, sharp structures are replaced by broader objects, governed by the width of $\delta_K^{(M)}$, which is typically $1/M$. Conversely, $\delta_K^{(M)}$ can be considered as an approximation of the delta function.

Equation (4.106) can be proved in a similar manner as (4.104). We consider

$$
\begin{aligned}
X &\stackrel{\text{def}}{=} \int_0^{2\pi} \; \delta_K^{(M)}(\varphi - \varphi')\; \tilde{f}(\varphi')\, d\varphi' \\
&= \frac{1}{2\pi} \; \int_0^{2\pi} \; \Big(\tilde{g}_0^{(M)} + 2 \sum_{m=1}^{M} \tilde{g}_m^{(M)} \cos(m(\varphi - \varphi')) \Big)\; \tilde{f}(\varphi')\, d\varphi' \; .
\end{aligned}
$$

Using (4.80), the integral for $m = 0$ evaluates to $\tilde{g}_0^{(M)}\, \mu_0$. The higher order terms are simplified exploiting trigonometric theorems

$$
\begin{aligned}
&\int_0^{2\pi} \; \cos\big(m(\varphi - \varphi')\big)\; \tilde{f}(\varphi')\; d\varphi' \\
&\qquad = \cos(m\varphi) \int_0^{2\pi} \cos(m\varphi')\, \tilde{f}(\varphi')\, d\varphi' + \sin(m\varphi) \int_0^{2\pi} \sin(m\varphi')\, \tilde{f}(\varphi')\, d\varphi' \; .
\end{aligned}
$$

Due to the symmetry $\tilde{f}(\varphi) = \tilde{f}(2\pi - \varphi)$ and $\sin(m(2\pi - \varphi')) = -\sin(\varphi')$, the second integral vanishes. Employing the relation $\cos(m(2\pi - \varphi')) = \cos(\varphi')$ for the first integral yields

$$\int_0^{2\pi} \cos(m\varphi')\,\tilde{f}(\varphi')\,d\varphi' = 2\int_0^{\pi} \cos(m\varphi')\,\tilde{f}(\varphi')\,d\varphi'$$

and therefore, as desired,

$$X = \tilde{g}_0^{(M)} + 2\sum_{m=1}^{M} \tilde{g}_m^{(M)}\,\mu_m\,\cos(m\varphi) = \tilde{f}^{(M)}(\varphi)\;.$$

The interesting conclusion from Equation (4.106) is that the truncated Chebyshev series corresponds to the convolution of the original function, or rather infinite series, with a polynomial kernel $\delta_K^{(M)}(\varphi)$. Of course, the

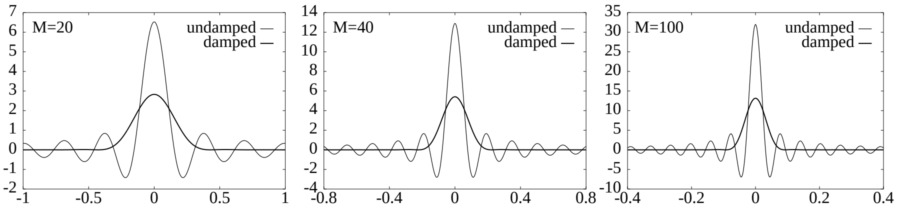

Fig. 4.9. Comparison between damped and undamped kernels for $20, 40$ and 100 Chebyshev moments. Notice the different scales used for the three plots! Approximate full widths at half maximum (FWHM) are 0.4, 0.2 and 0.05, respectively.

quality of the reconstruction depends essentially on the kernel. Representative polynomial kernels are displayed in Fig. 4.9 for different cut-off values $M = 20, 40, 100$. For the undamped case, $g_m^{(M)} = 1$ pronounced ringing is observed, obviously violating the positivity request. The impact of these oscillations on the convolution is demonstrated in Fig. 4.8 for the step function. The dotted lines represent the truncated Chebyshev series without damping. Pronounced oscillations appear in the vicinity of the discontinuities. The typical features of Gibbs-oscillations are apparent: Increasing M does not lead to a monotonic point-wise convergence. The number of oscillations increases instead, while the amplitudes are not affected. On the other hand, it is visible to the naked eye that window-averages approach the correct result and the size of the window decreases with increasing M. This motivates in hindsight the convolution with a blurring kernel, the size of which should ideally decrease with $1/M$. The discussion about optimal kernels can be found in the standard literature on approximation theory. The optimal kernel has to fulfill the following requirements:

1. positivity: $\delta_K^{(M)}(\varphi) \geq 0$ to enforce positivity of $\tilde{f}^{(M)}(\varphi)$ and hence of $f^{(M)}(x)$.
2. unbiased: $\int_{-\pi}^{\pi} \varphi \, \delta_K^{(M)}(\varphi) \, d\varphi = 0$
3. norm-conservation: $\int_{-\pi}^{\pi} \delta_K^{(M)}(\varphi) \, d\varphi = 1$.
4. Optimize resolution, i.e. minimize the variance $\int_{-\pi}^{\pi} \varphi^2 \, \delta_K^{(M)}(\varphi) \, d\varphi$

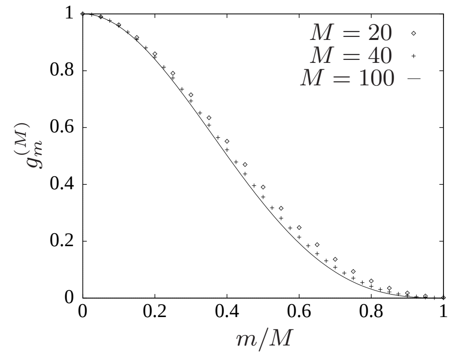

Fig. 4.10. Damping coefficients $g_m^{(M)}$ according to Silver & Röder for the values $M = 20, 40, 100$.

By construction the kernel in (4.105) is a polynomial of degree M. A sufficient condition for positivity is the positivity of the kernel-polynomial $\delta_K^{(M)}(\Phi) \geq 0$. Here, the trigonometric representation appears to be particularly useful. The positivity constraint is more difficult to ensure in the $x-$representation. The norm is given by the prefactor of $T_0(x)$, hence norm-conservation implies $g_0^M \equiv 1$. As a consequence of the conditions, the kernel converges to a Dirac δ-distribution in the limit $M \to \infty$. This property is shared by the original undamped kernel.

Ideal damping coefficients, as derived in [15, 16], are given by the Jackson coefficients

$$g_m^M = \sum_{\nu=0}^{M-m} a_\nu \, a_{\nu+m} \; , \tag{4.107}$$

which leads to the apparently positive kernel

$$\delta_K^{(M)}(\varphi) = \left| \sum_{\nu=0}^{M} a_\nu \; e^{i\nu\varphi} \right| \; .$$

The coefficients a_ν, which minimize the variance in φ, subject to the normalization constraint are given by

$$a_\nu = \frac{U_\nu(\lambda)}{\sqrt{\sum_{\nu'=0}^{M} U_{\nu'}^2(\lambda)}} \,, \tag{4.108}$$

and $U_\nu(\lambda)$ are Chebyshev polynomials of the second kind

$$U_\nu(\lambda) = \frac{\sin((\nu+1)\,\varphi_\lambda)}{\sin(\varphi_\lambda)} \quad ; \quad \cos(\varphi_\lambda) = \lambda \,; \quad \varphi_\lambda = \frac{\pi}{M+2} \tag{4.109}$$

These kernels are sketched as solid lines in Fig. 4.9. Obviously, they fulfill the desired conditions. The reconstruction of the step function provided by the optimal kernels is depicted in Fig. 4.8.

The Jackson coefficients are plotted in Fig.4.10 as function of m/M. We observe that the g's smoothly tend from 1 to 0 and that $g(m/M$ approaches a universal curve.

KPM is a linear and hence fast method but it is also an ad-hoc scheme. An alternative, consistent approach, based on the rules of probability theory, has also been proposed by Silver and Röder [16]. It employs the entropic prior and corresponds to the maximum entropy moment method earlier proposed by Bretthorst[18] and applied to fusion-plasma problems in [19].

As pointed out by Silver et al., KPM allows an immediate computation of the partition-function

$$Z = \sum_i e^{-\beta\varepsilon_i} = e^{-\beta b} \int_{-1}^{1} e^{-\beta a\,\varepsilon}\, \tilde{\rho}(\varepsilon)\, d\varepsilon \,,$$

where (4.81) and (4.82) have been exploited. Inserting the Chebyshev-expansion of the density of states yields

$$\begin{aligned} Z = \pi\, e^{-\beta b} \Big(& \mu_0 \int_{-1}^{1} e^{-\beta a\,\varepsilon}\, T_0(\varepsilon)\, \frac{1}{\pi\sqrt{1-\varepsilon^2}}\, d\varepsilon \,+ \\ & 2 \sum_{n=1}^{M} \mu_n \int_{-1}^{1} e^{-\beta a\,\varepsilon}\, T_n(\varepsilon)\, \frac{1}{\pi\sqrt{1-\varepsilon^2}}\, d\varepsilon \Big) \\ = \pi\, e^{-\beta b} \Big(& \mu_0\, I_0(-\beta a) + 2 \sum_{n=1}^{M} \mu_n\; I_n(-\beta a) \Big) \,. \end{aligned}$$

The sum over the Bessel-functions of the first kind I_m converges rapidly.

The kernel-polynomial method has also been generalized for the computation of spectral functions[20]. An application to dielectric functions is discussed in[21]. The generalizations are very interesting but straight forward and they go beyond the scope of this book. For a comparison of KPM and the Lanczos approach we refer the reader to [15].

1. J. Hubbard, Phys.Lett. **3**, 77 (1959).
2. J. Hubbard, Proc. Roy. Soc. **A 276**, 238 (1963).
3. V. Emery, Phys.Rev.Lett. **58**, 2794 (1987).
4. F.C.Zhang and T. Rice, Phys.Rev. **B 37**, 3795 (1988).
5. T. Rice, Helv. Phys. Acta **63**, 336 (1990).
6. P.W.Anderson, Phys.Rev. **124**, 41 (1961).
7. P. Lee *et al.*, Comments Condens.Matter **12**, 99 (1986).
8. P.Fulde, J.Keller, and G.Zwicknagel, Solid State Physics **41**, 1 (1988).
9. P.A.Lee *et al.*, Comments Condens. Matter Phys. **12**, 99 (1986).
10. A. Harris and R. Lang, Phys.Rev. **157**, 295 (1967).
11. T. Matsubara and H.Matsuda, Prog. theor. Phys. **16**, 569 (1956).
12. M. Z. W. von der Linden and P. Horsch, Phys. Rev. B **40**, 7435 (1989).
13. M. Lieb, Schultz, Annals of Physics **16**, (1961).
14. M. Lieb, Journal of Mathematical Physics **749**, (1962).
15. R. N. Silver, H. Roeder, and A. F. V. andl J. D. Kress, Journal of Computational Physics **124**, 115 (1996).
16. R. N. Silver and H. Roeder, cond–mat/ 9703229 (1997).
17. C. Lanczos, *Applied Analysis* (Dover Publication Inc., New York, 1993).
18. *Bayesian Spectrum Analysis and Parameter Estimation*, edited by G. Bretthorst (Springer Press, Berlin, Heidelberg, 1988).
19. W. Eckstein, W. von der Linden, and V. Dose, Nucl. Instrum. and Methods in Phys. Res. **B 95**, 14 (1994).
20. R. N. Silver and H. Roeder, Int.J.mod.Phys.C **5**, 735 (1994).
21. L.-W. Wang and A. Zunger, Phys.Rev.Lett. **73**, 1039 (1994).